Molecular Phylogenetics and Evolution 204 (2025) 108280

Contents lists available at ScienceDirect

Molecular Phylogenetics and Evolution

journal homepage: www.elsevier.com/locate/ympev

Genomic data support reticulate evolution in whiptail lizards from the Brazilian Caatinga

Felipe de M. Magalhães [a,b,*], Eliana F. Oliveira [c], Adrian A. Garda [d], Frank T. Burbrink [e], Marcelo Gehara [a]

[a] Department of Earth and Environmental Sciences, Rutgers University, Newark, NJ, USA
[b] Programa de Pós-Graduação em Ciências Biológicas, Centro de Ciências Exatas e da Natureza, Universidade Federal da Paraíba, João Pessoa, Paraíba, Brazil
[c] Instituto de Biociências, Universidade Federal de Mato Grosso do Sul, Campo Grande, Mato Grosso do Sul, Brazil
[d] Laboratório de Anfíbios e Répteis (LAR), Departamento de Botânica e Zoologia da Universidade Federal do Rio Grande do Norte, Natal, Rio Grande do Norte, Brazil
[e] Department of Herpetology, The American Museum of Natural History, New York, NY, USA

ARTICLE INFO

Keywords:
Ameivula
Ancient introgressive hybridization
Mitochondrial capture
Mitonuclear discordance
Multi-species network coalescent
Species delimitation
Ultraconserved elements

ABSTRACT

Species relationships have traditionally been represented by phylogenetic trees, but not all evolutionary histories fit into bifurcating divergence models. Introgressive hybridization challenges this assumption by sometimes [or maybe often] leading to mitochondrial introgression, wherein one species' mitochondrial genome is entirely replaced by another's (mitochondrial capture). Such processes result in mitonuclear discrepancies, complicating species delimitation and phylogenetic inference. In our study, we used ultraconserved elements (UCE) and mitogenomic data to investigate the evolutionary history of the *Ameivula ocellifera* complex, a group of South American whiptail lizards widely distributed in semiarid environments of the Caatinga Domain in Brazil. We examine mitonuclear discordances, assessing reticulate evolution, evaluating species limits, and testing for adaptive mitochondrial capture that could explain higher introgression in the mitochondrial genome compared to nuclear DNA. Our findings support the occurrence of an ancient reticulation event during the diversification of these lizards, driven by introgressive hybridization, leading to mitochondrial capture, and explaining mitonuclear discrepancies. Overall, we did not find clear evidence of positive selection across mitochondrial protein-coding genes suggesting adaptive mitochondrial capture of individuals with introgressed mtDNA. Thus, the genetic diversification and mitogenome evolution could be neutral, with selection against hybridization in the autosomal loci only, or even mediated by mitonuclear incompatibilities. Analyses of mtDNA genomes alongside network and species delimitation methods were crucial for identifying and validating individuals with introgressed mtDNA as a distinct species, demonstrating the potential of genome sampling, and using innovative analytical techniques for elucidating speciation processes in the presence of introgressive hybridization.

1. Introduction

Speciation is generally initiated by population divergence with reduction in gene flow between lineages (Mayr 1963; de Queiroz 2007). From a spatial perspective, this process of divergence is categorized in three main types: allopatric, parapatric, and sympatric. From a genetics perspective, it can be neutral or adaptative (Wu 2001). Speciation though is likely complex and may involve ecological adaptation and/or alternating periods of isolation and contact, showing contemporary or past horizontal connections between branches of a phylogeny (Abbott et al. 2013; Mallet et al. 2016; McGee et al. 2020). As more genomic datasets are generated, it is now common to find species persisting as distinct given gene flow (Mallet et al. 2016; Cahill et al. 2018; Wang et al. 2020; Burbrink et al. 2021). Introgression can introduce new variants that potentially increase the fitness of individuals in a population (The Heliconius Genome Consortium 2012; Tigano and Friesen 2016; Jones et al. 2018). However, in the absence of selection, introgression may homogenize diverging populations. Thus, some cases of hybridization represent natural experiments to understand non-neutral evolutionary forces in the speciation process.

One genomic region that is commonly investigated and can undergo adaptive introgression is the mitochondrial DNA (mtDNA; da Fonseca

* Corresponding author at: 195 University Ave, Boyden Hall, Room 435, Newark, NJ 07102, USA.
E-mail address: felipemm17@gmail.com (F.M. Magalhães).

https://doi.org/10.1016/j.ympev.2024.108280
Received 1 April 2024; Received in revised form 16 December 2024; Accepted 21 December 2024
Available online 24 December 2024

et al. 2008; Castellana et al. 2011; Boratyński et al. 2014). Introgression may cause the partial or complete replacement of the mitochondrial genome of one species by that of another, commonly referred to as mitochondrial capture (mt-cap; Hill 2019). Together with incomplete lineage sorting (ILS), some studies suggest mt-cap as one of the main causes of mitonuclear discordances (Ballard and Whitlock 2004; Toews and Brelsford 2012). Mitochondria are vital components of eukaryotic cells as they are directly involved in oxygen metabolism and energy production (Das 2006; Breton et al. 2014). In general, the mtDNA is expected to evolve under purifying (negative) selection, where deleterious mutations are selected against to maintain protein functionality (Castellana et al. 2011; Shtolz and Mishmar 2019). Additionally, mitochondrial and nuclear genes (nuDNA) involved in energetic metabolism are constrained to coevolve in order to maintain efficient energy production through the oxidative phosphorylation (OXPHOS) enzymes system (Rand et al. 2004; Bar-Yaacov et al. 2012; Hill 2015). The strong functional link between nuclear and mitochondrial genes results in natural selection against hybrids and potentially restricts gene flow among *meta*-populations (Ellison and Burton 2008; Gershoni et al. 2009; Burton and Barreto 2012; Sloan et al. 2017; Telschow et al. 2019), which may ultimately drive divergence and speciation (Gershoni et al. 2009; Bar-Yaacov et al. 2015; Hill 2015; Henault and Landry 2016). Conversely, positive selection on mtDNA codons and genes suggests that changes have functional effects, possibly in relation to metabolic efficiency and physiological adaptations to environmental constraints (Romero et al. 2016; Lamb et al. 2018). Selective pressures acting on mtDNA may also drive discordances with biogeographic patterns obtained from nuDNA (Toews and Brelsford 2012). Therefore, understating how selection is driving mitochondrial differentiation can help clarify the speciation process and better inform species delimitation (Bar-Yaacov et al. 2015; Morales et al. 2018; Bernardo et al. 2019; Shults et al. 2022).

Mitochondrial DNA has been traditionally the marker of choice to assess phylogeographic structure and species limits (Hebert et al. 2003). Generally, species delimitation studies contrast the genetic structure of mtDNA and nuDNA (when discordant) as opposing evidence to determine species limits, and generally favor the solution supported by genomic data (Pedraza-Marrón et al. 2019; Shults et al. 2022). Undoubtedly, the increasing ease of collecting genome-scale data is providing more refined information about species boundaries, while relying on the mitochondrial genome alone can often lead to erroneous species delimitations (Ballard and Whitlock 2004), especially when introgression occurs among diverging lineages (Dinca et al. 2019; Chan et al. 2021; Ortiz et al. 2021). Hence, introgressive hybridization and adaptive mt-cap represent challenges for species discovery and delimitation methods given that they violate the assumptions of a bifurcating divergence model. Moreover, species discovery and validation methods (e.g., Roux et al. 2016; Jackson et al. 2017; Leaché et al. 2019) yield results that are based on the predominant genomic signal, which can be misleading depending on the history of introgression (Harrison and Larson 2014). For instance, only a few regions of the genome might be important for adaptation, being under strong natural selection (Yeaman and Whitlock 2011; Andrew and Rieseberg 2013). Those regions tend to remain distinct even in the presence of the dominant signal of introgression (Renaut et al. 2013; Martin et al. 2019).

In recent years, the development of new analytical methods that model horizontal connections among branches of a phylogeny (i.e., phylogenetic networks) has allowed a more comprehensive understanding of species evolution (Solís-Lemus et al. 2017; Wen and Nakhleh, 2018), simultaneously enlightening the processes that generate mitonuclear discordance (Thanou et al. 2020; Cairns et al. 2021; Barley et al. 2022). Network methods have allowed researchers to estimate deep time reticulations on trees (Burbrink and Gehara 2018) and solve some taxonomic and systematic uncertainties that cannot unambiguously be untangled using mtDNA alone, or in combination with a few nuclear loci (Quattrini et al. 2019; Mason et al. 2019; Stull et al. 2020; Cairns et al. 2021; Esquerré et al. 2022). Such advances prompted an increasing number of cases reporting reticulate evolution and introgression across many biological groups, thus underscoring an important evolutionary mechanism in natural populations (Abbot et al. 2013; Meier et al. 2017; Payseur and Rieseberg 2016; Taylor and Larson 2019; Patton et al. 2020).

Along the Caatinga Domain in northeastern Brazil, the largest xeric and seasonally dry tropical forest nucleus of South America (Silva et al. 2017), a challenging case of species delimitation is that of *Ameivula* whiptail lizards. These lizards exhibit conspicuous coloration patterns and extensive morphological variation suggesting multiple unrecognized species (Rodrigues 2003), but efforts to establish species limits with genetic datasets have only recently been attempted (Oliveira et al. 2015; Arias et al. 2018), with different studies proposing different numbers of taxa. Based on dense geographic sampling using one mitochondrial and four nuclear loci analyzed with coalescent-based models, Oliveira et al. (2015) delimited two main lineages (*A. ocellifera* and *A. xacriaba*) that diverged with gene flow under a parapatric speciation model. Their data show that *A. ocellifera* was genetically homogeneous and broadly distributed in Caatinga. Later, Arias et al. (2018), using spatially sparse sampling and three mitochondrial and one nuclear locus analyzed with standard phylogenetic methods, uncovered more genetic diversity within the Caatinga. They recognized five species (*A. ocellifera*, *A. confusioniba*, *A. nigrigula*, *A. pyrrhogularis*, and *A. xacriaba*), plus a candidate lineage related to *A. ocellifera*. They also pointed out that morphological and genetic evidence (dominated by mitochondrial data) often disagree on the validity of some species they recognized (e.g., *A. confusioniba* and *A. mumbuca*), but did not discuss which processes may lead to these incongruences. We hypothesize that gene flow between lineages (Oliveira et al. 2015) or introgression (as shown for North American whiptail lizards; Barley et al. 2022) could be masking the diversification history of this group, creating a confounding and contrasting scenario of species delimitation. Furthermore, because previous studies have underscored the significance of environmental gradients between the neighboring Caatinga and Cerrado regions in the diversification process of Neotropical lizards (Werneck et al. 2012; Oliveira et al. 2015), adaptive introgression across ecotonal and elevational zones might be at play.

To test these hypotheses, we analyzed thousands of ultraconserved elements (UCE) loci and the mitochondrial genome of 50 samples comprising 43 localities. We used phylogenetic network methods, divergence time estimates, coalescent simulations, and selection tests on mitochondrial protein-coding genes to disentangle a complex history of diversification and to understand the origin of genomic discordances involving ancient introgression with mitochondrial capture by one species. Our study reconciles the contrasting information provided by mitochondrial and nuclear genomes to better understand a complex speciation process.

2. Material and methods

2.1. Sampling, Library Prep, and sequencing

We sampled a total of 50 individuals covering the geographic range of the *Ameivula ocellifera* complex (Fig. 1), which includes *A. ocellifera*, *A. pyrrhogularis,* and three species that occur within the Caatinga Domain and/or adjacent Cerrado areas: *A. confusioniba*, *A. nigrigula*, and *A. xacriaba* (see Supplementary Table S1). We extracted and purified genomic DNA from tissues using Qiagen DNeasy Blood and Tissue Kits (Qiagen Inc.) and quantified extractions using a Qubit 2.0 fluorometer (Life Technologies, Inc.) to verify DNA quality. We used services from RAPiD Genomics (https://www.rapidgenomics.com/services/) to generate 5,472 baits and to sequence 5,060 UCE loci following the protocols from Faircloth et al. (2012) and Sun et al. (2014). Pooled libraries were then sent to the University of Florida ICBR Facility for 100 bp paired-end sequencing on an Illumina HiSeq 3000. Using dual-

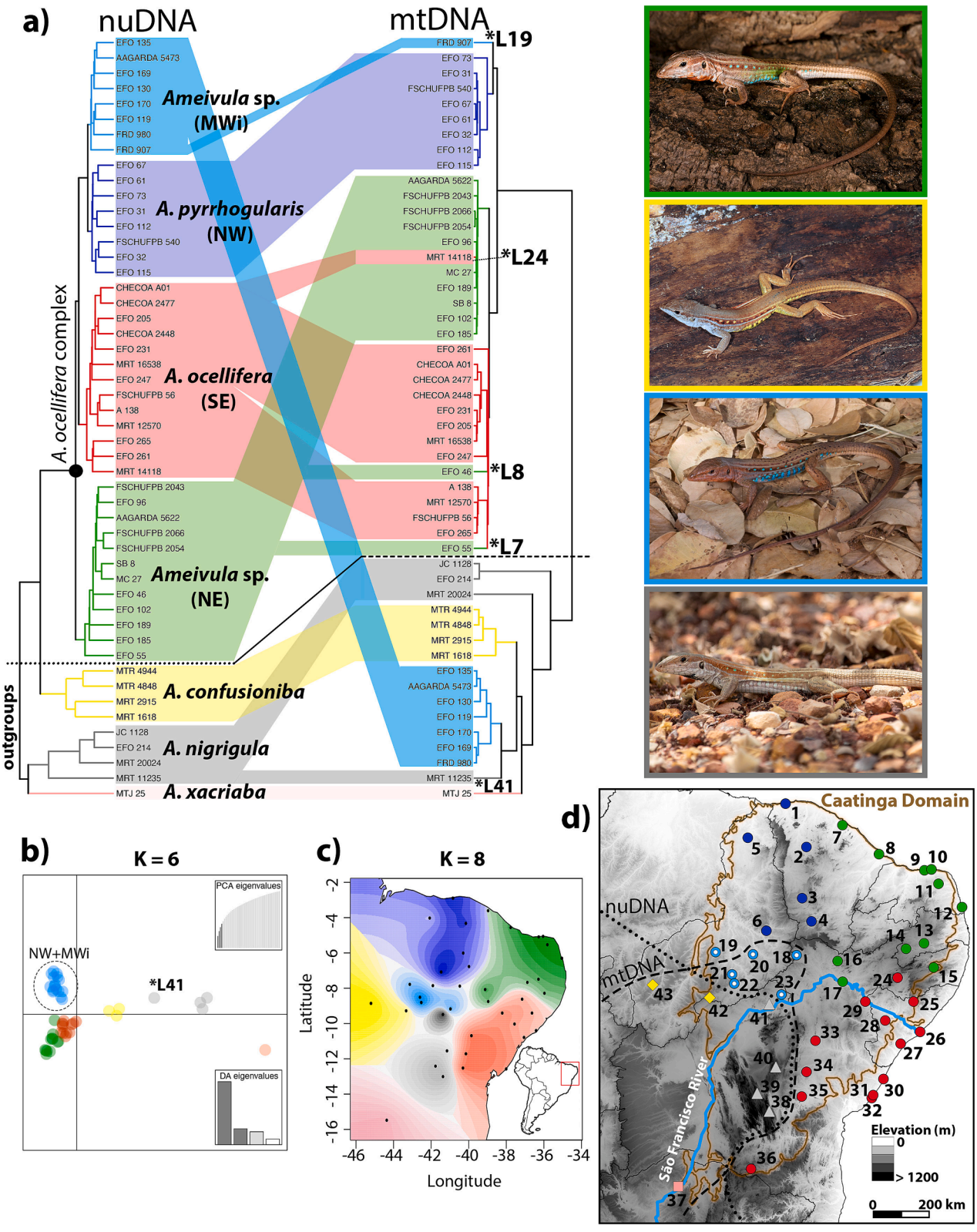

Fig. 1. a) Concatenated nuclear (nuDNA) tree based on 2,560 UCE loci and complete mitogenome (mtDNA) tree for 50 *Ameivula* samples used in this study. Different colors correspond to different lineages/species based on DAPC and TESS3 results. The black dotted line in the nuDNA tree separates the outgroups from the *Ameivula ocellifera* complex, while the dashed line in the mtDNA tree highlights the close relationship between MWi lineage and outgroups. The samples with *L denotes individuals recovered as paraphyletic in the mtDNA, while the number indicates its geographic location in the map. Each species is color coded to the lizard images on the side; b) DAPC results. Scatterplot showing the first two principal components from DAPC with best K = 6. Each cluster is indicated by a different color and each point is an individual. The eigenvalues retained in principal component analysis (PCA) and discriminant analysis (DA) are indicated; c) TESS3 results. Geographic maps of ancestry coefficients using K = 8 ancestral populations. Black dots represent the sample locations and each cluster is indicated by a different color; and d) Distribution of samples used in this study, totalizing 43 localities (more details in Supplementary Table S1). Different colors correspond to different lineages. Black dotted and dashed lines refer to lines of the nuDNA and mtDNA trees, depicting mitonuclear incongruence of the MWi lineage.

indexed barcodes, multiple clean-ups, and quality control steps, the amount of reads that mapped to impossible index combinations was low (average index hopping rate = 0.2 %) (Sinha et al. 2017.).

2.2. Mitochondrial genome assembly and analyses

We identified and assembled the mitochondrial genome from off-target sequencing reads by mapping the illumiprocessor cleaned reads to a mitogenome reference of *Callopistes maculatus* (GenBank accession number AB176924), which is the closest relative (Teiidae family) to our ingroup with a complete mitogenome available on GenBank during the time we surveyed for mitogenomes (2021). We followed the pipeline and scripts provided by Evan Twomey available in GitHub (https://github.com/jasonleebrown/UCE_phyluce_pipeline/blob/master/README.md#mitogenome-pipeline). This pipeline first uses BWA (Li and Durbin 2009) to construct the index for the reference genome (the "index" option) and BWA-MEM algorithm to align both fastq.gz reads with the reference genome ("mem" option), which are stored in SAM format. Samtools v1.1.19 (Danecek et al. 2021) was then used to convert from SAM to BAM files and, lastly, ANGSD v0.934 (Korneliussen et al. 2014) was used to extract variants/sequences from the BAM files previously created and export as FASTA. Because the available reference mitogenome was from a distantly related species, we used EMBOSS v6.6 (Rice et al. 2000) to create a consensus sequence of all our *Ameivula* samples and repeated the baiting and alignment pipeline to retrieve mitogenomes with fewer missing data. Final annotation of the mitogenomes was performed using Geneious R9 (Kearse et al. 2012). We also inspected protein-coding regions for proper amino acid translation, confirmed that there are no internal stop codons, and manually eliminated the D-loop region from the alignment. To evaluate mitochondrial sequence authenticity, we compared the ribosomal genes retrieved through this pipeline with the 12S gene sequences published by Oliveira et al. (2015). The annotated and partitioned mitogenomes are available via the Mendeley Digital Repository (https://doi.org/10.17632/srm6w345sr.1; see also Supplementary Table S1).

We used the resulting alignment to construct a mitogenome dataset using *Callopistes maculatus* as our outgroup. The final concatenated alignment of 15,277 bp was split into five partitions according to transcript type (tRNA: 1,575 bp; rRNA: 2,480 bp; protein-coding mRNA: 11,223 bp) and all protein-coding genes (PCGs) subdivided into codon position (COD-p1, COD-p2, and COD-p3, with 3,741 bp each). To date the divergences between all our *Ameivula* samples (total of 50 individuals), we used the estimates of Burbrink et al. (2020) to constraint the divergence between the last common ancestor of *Ameivula* and *Callopistes*, which was given as a lognormal prior with mean (M) of 71.49 Ma and standard deviation (S) of 0.025. This age constraint was retrieved from a fossil calibrated phylogenetic tree estimated with genomic-scale data for Squamata, being the most reliable calibration point available for our ingroup. We also used the 12S substitution rate of 5.11 x 10^{-3} substitutions/site/Ma estimated for the Teiidae family (Oliveira et al. 2015) as a prior for the clock rate. We ran three independent analyses in BEAST2 v2.6.6 with a relaxed uncorrelated lognormal clock, a birth–death tree model, for 50 x 10^{6} MCMC generations sampling every 5,000 iterations, discarding the first 10 % of samples as burn-in. The best model of nucleotide substitution for each partition was co-estimated during the analysis using BEAST Model Test v1.2.1 (Bouckaert and Drummond 2017) implemented in the BEAST2 package. We examined convergence trace plots in TRACER v1.7 (Rambaut et al. 2018) to ensure that all parameters ESS > 200 and combined logs from distinct runs with LogCombiner (BEAST2 package). To determine if missing data may have any effect on tree topology and node support, we removed seven individuals that had more than 50 % of missing data and used GBLOCK v0.91b (Castresana 2000) to exclude potentially poorly aligned positions and missing data blocks of the mitogenome alignment. We then used ModelFinder to infer the best-fit model of substitution and IQ-TREE 2 to infer a maximum likelihood tree with 1,000 bootstrap replicates to assess node support.

2.3. UCE assembly and SNP data

We assembled UCEs for each sample using a modification of the Phyluce pipeline (Faircloth 2016). We first ran a de novo assembly for each sample with VelvetOptmiser.pl (Velvet v1.2.1; Zerbino and Birney 2008) using 65 and 75 as *hashs* and *hashe* parameters, respectively, and used the total number of base pairs in all contigs as an optimization function for coverage cutoff. After the de novo assembly, we proceeded with the standard Phyluce pipeline. We used the scripts 'phyluce_assembly_get_match_counts' and 'phyluce_assembly_get_fastas_from_match_counts' to match contigs of each sample to reference probes using the R platform (R Core Team 2021). Then, we used the Burrows-Wheeler Aligner (BWA) v0.7.12 (Li and Durbin 2009) to map reads to the de novo assembled contigs and used Picard Tools v1.119 (https://broadinstitute.github.io/picard/) to exclude PCR duplicates. We used The Genome AnalysisToolkit (GATK) v3.6.0 (McKenna et al. 2010) to call, realign, and maskindels, call and annotate single nucleotide polymorphisms (SNP), and perform read-backed phasing. Next, we used the 'add_phased_snps_to_seqs_filter.py' of the seqcap_pop pipeline (Harvey et al. 2016) to generate sample specific FASTA files. We then combined, aligned, and trimmed all samples into one FASTA alignment per UCE using a custom R script. This script used MUSCLE to align sequences and exclude individuals with very short sequences. To do that, we calculated for each UCE alignment the distribution of sequence lengths and excluded all sequences below the 25 % quantile. We also created custom R scripts to convert phased UCE alignments to VCF format. For each polymorphic locus, we identified the variable sites using the seg.sites function of the pegas R package and we randomly sampled one variable site per locus to eliminate biases due to linkage of SNPs. We further filtered loci and individual missing data using the R package dartR (Gruber et al. 2018). Loci that were invariant, non-biallelic, or absent from > 60 % of samples were removed. Because missing data can influence population assignment, samples with > 60 % missing data were also removed. The resulting unlinked SNP data set was used to generate input files for downstream analyses. Further re-filtering was made when a different set of samples was used in analyses. Raw FASTQ files for all samples were uploaded to the NCBI sequence read archive (PRJNA1197672; Table S1). Per locus phased alignments are available via the Mendeley Digital Repository (https://doi.org/10.17632/srm6w345sr.1).

2.4. Genetic structure

To assess if populations of the *Ameivula ocellifera* complex harbor potentially cryptic lineages, we used a Discriminant Analysis of Principal Components (DAPC; Jombart et al. 2010) in the R package adegenet v2.1.2 (Jombart 2008), which sequentially estimates K-means for clustering and selects the best fit to infer genetic clusters in the absence of prior group identification. We first transformed the SNP data using principal component analysis (PCA) by choosing a large number of PC axes (n = 100), then picking the number of discriminant functions yielding large F-statistics (>2000) and selected the number of genetic clusters based on the number of PC axes that minimized the Bayesian information criterion (BIC) score. Because using a large number of the PCs may yield arbitrary solutions, we estimated the optimal a-score, which measures this bias by calculating the difference between the actual cluster assignment probabilities and randomly assigned probabilities (predicting 4–8 PCs). We also assessed population structure using TESS3r R package to estimate admixture for each species pair using SNPs and geographic data (Caye et al. 2018), which accounts for geographic distance among samples to estimate ancestry coefficients. We ran the TESS3 function with 20 replicates for K equals 1 to 15 using default parameters. Each of these methods (i.e., DAPC and TESS3) use different assumptions for grouping individuals and we compared congruence

among them.

2.5. Concatenated tree

We used maximum-likelihood (ML) analysis of concatenated data as an initial estimate of phylogenetic relationships with nuclear data. We generated a concatenated gene tree using all UCE loci for all individuals we sequenced. This dataset consisted of 2,560 loci and a total of 717,415 base pairs. The automatic model selection method was used to infer the best-fit model of substitution (Kalyaanamoorthy et al. 2017), and a maximum likelihood gene tree was then inferred with 1,000 ultrafast bootstrap replicates to assess node support in IQ-TREE 2 (Minh et al. 2020).

2.6. Species delimitation

One of the clusters delimited by TESS showed an incongruence between mitochondrial and nuclear genomes related to its placement within the *Ameivula ocellifera* complex, potentially because of introgression, also exhibiting two distinct mitochondrial genomes. To test among competing delimitation models and assure that the mid-western cluster (or MWi) can be validated as an independently evolving species using SNP data, we conducted a species delimitation analyses using the Bayes Factor Delimitation (BFD) method (Leaché et al. 2014) in SNAPP v1.5.2 (Bryant et al. 2012) package in BEAST2 v2.6.6 (Bouckaert et al. 2014). The competing delimitation models were derived from previous taxonomic proposals (i.e., Oliveira et al. 2015; Arias et al. 2018) and different combinations of the exploratory analyses of population structure of the genomic data collected here. Therefore, we tested four species delimitation models: (a) four species based on TESS3 results (which validated MWi with mtDNA introgression); (b) three species based on DAPC results (lumping midwestern and northwestern clusters); (c) two valid species represented by *A. pyrrhogularis* (lumping midwestern and northwestern clusters) and *A. ocellifera* (individuals from northeastern and southeastern clusters lumped), which corresponds to the current taxonomic scenario according to Arias et al. (2018); and (d) the *A. ocellifera* complex represents a single taxon and *A. pyrrhogularis* would be a synonym of *A. ocellifera* (as proposed by Oliveira et al. 2015).

While it may be ideal to include all sequenced specimens, the Bayesian framework implemented in SNAPP would make the empirical analysis and posterior predictive simulations computationally intractable. We included five individuals with less missing data per potential species (for a total of 20 ingroup samples; see Supplementary Table S1 for individual samples used in this analysis) plus the outgroup taxon *Ameivula confusioniba* so that the single *A. ocellifera* species model could be evaluated. SNAPP requires that at least one individual is sampled at each locus for every species set. Therefore, we filtered 651 SNPs assuring that reassigning individuals between species sets would not change the number of sites among competing models. We set forward and reverse mutation rates to 1. We applied a gamma distribution ($\alpha = 2$, $\beta = 200$) for the speciation rate (λ) prior and the snapprior was set to $\alpha = 1$, $\beta = 250$, and $\kappa = 1$ (following Leaché et al. 2014). To test the four alternative species delimitation models, we used a stepping-stone analysis with the PathSampleAnalyser with 72 steps and a chain length of 200,000, burnin percentage at 50 %, and a preburnin of 10,000. Convergence was assessed by examining log plots in TRACER v1.7 (Rambaut et al. 2018), ensuring that all ESS values > 200. We ranked and compared the resulting marginal likelihood values using Bayes factors (BF; Kass and Raftery 1995). The strength of support from BF comparisons of competing models can be evaluated as follows: $0 < BF < 2$ is not worth more than a bare mention, $2 < BF < 6$ is positive evidence, $6 < BF < 10$ is strong support, and $BF > 10$ is decisive.

Because the SNAPP model is migration-free and only produces strictly bifurcating trees, we used posterior predictive simulations to test if these data are a good fit to the multispecies coalescent model (MSCM) implemented in SNAPP. We used the R package P2C2M.SNAPP (Duckett et al. 2020) to conduct these simulations. P2C2M.SNAPP was used to generate 100 posterior predictive datasets that mirrored our empirical data in numbers of samples and sites; these simulations were then run in SNAPP. To compare the posterior distribution from the empirical data to the predictive distribution, we used all three summary statistics implemented in *P2C2M.SNAPP*: the Robinson-Foulds tree distance (RF), the standard deviation of maximum likelihoods of posterior trees, and pairwise FST outliers.

To further determine whether putative species boundaries corresponded to species-level divergences, we used a heuristic species delimitation using the genealogical divergence index (*gdi*; Jackson et al. 2017). To calculate *gdi*, we used the following equation: $gdi = 1\text{–}e^{-2\tau/\theta}$ (Jackson et al. 2017; Leaché et al. 2019), where population A is distinguished from population B using the equation $2\tau_{AB}/\theta_A$, while $2\tau_{AB}/\theta_B$ is used to differentiate population B from population A. We used BPP v4.3.8 (Flouri et al. 2018) to estimate the parameters τ and θ (A00 analysis) with thetaprior = 3 0.002 *e* and tauprior = 3 0.004 and the species tree topology estimated using SNAPP as the guide tree. We used the same individuals present in the BFD analysis (individuals with less missing data) plus two individuals of *Ameivula nigrigula* and *A. confusioniba*, and one individual of *A. xacriaba* (outgroup species). For the analysis to be computationally tractable, we filtered our phased UCE alignments to include only loci with parsimony informative sites above two (880 loci). Four separate runs were performed [100,000 Markov-Chain Monte Carlo (MCMC) iterations each] and converged runs were concatenated to generate posterior distributions for the multispecies coalescent parameters. Populations were considered distinct species when *gdi* values were ≥ 0.7; low *gdi* values (≤ 0.2) indicated that two populations belonged to the same species; values of $0.2 \leq gdi \leq 0.7$ indicated ambiguous species status, therefore requiring that additional information was needed to ascertain the species status (Pinho and Hey 2010; Jackson et al. 2017).

2.7. Phylogenetic networks

Our earlier results indicate a mitonuclear discordance among species in the *Ameivula ocellifera* complex suggesting that a reticulation event (i.e., mitochondrial capture) might have occurred, although ILS might also be a factor contributing to discordance (see below the topic *Introgression*). To understand if the evolution of these lizards can be explained by reticulated trees (instead of fully bifurcating), we used the multi-species network coalescent approach SNaQ (Solís-Lemus et al. 2017), which calculates the maximum pseudolikelihood of a network from four-taxon concordance factors (CFs) as implemented in the *PhyloNetworks* Julia package (https://github.com/crsl4/PhyloNetworks.jl). Before the analysis, we filtered our UCE alignment data to include only loci with full taxon representation (all seven species) that have at least one parsimony informative site (542 loci), also randomly retaining one sequence/allele per species per loci. All filtering was made using custom R scripts. To generate the CFs, we used BUCKy v1.4.4 (Ané et al. 2007) through the TIRC pipeline (Stenz et al. 2015; https://github.com/nstenz/TICR). The TICR pipeline was initiated by running MrBayes for every UCE locus using the HKY nucleotide substitution model, with a MCMC of 400,000 generations with two chains, a temperature of 0.20, and a swapping frequency of 10. We sampled parameters every 100 generations and discarded 20 % as burn-in. We then used the MrBayes output trees as inputs for BUCKy under default parameters to generate a four-taxon concordance factor table. We also used the resulting set of gene trees from the above pipeline as input to a species tree inference in ASTRAL v5.7.7 (Zhang et al. 2018), which we used as a starting bifurcating tree. Phylogenetic networks were reconstructed with the snaq! function in PhyloNetworks using CFs table and running 10 independent analyses and inferring networks with the number of hybridization events (hmax) ranging from 0 to 5. The best-fit number of reticulation events was inferred by plotting likelihood scores for each run, varying hmax, and observing the point where adding additional reticulations did

not largely improve the pseudolikelihood score (a slope heuristic approach; Solís-Lemus et al. 2017). After defining the number of reticulations, we assessed their support using 100 bootstrap replicates which were summarized using PhyloNetworks.

TreeMix v1.13 was used (Pickrell and Pritchard 2012) to estimate a maximum likelihood topology and infer gene flow between all *Ameivula* species from Caatinga validated previously. The analysis included all samples that passed missing data thresholds (see methods above), including only biallelic sites. For SNPs with missing allele counts in ≥ 1 lineage/species we removed them from the input data set prior to analysis (1,308 SNPs retained). To model uncertainty in the sample covariance matrix, we implemented block jackknife resampling (−k flag) across groups of 100 unlinked SNPs. We used the clade formed by *Ameivula confusioniba*, *A. nigrigula*, and *A. xacriaba* to root the tree according to the topology of the PhyloNetworks and ASTRAL species tree, as required by TreeMix. We tested for one to ten migration events (*m*) to the tree and each analysis included 1,000 bootstrap replicates. We ran ten replicates for each value of *m*, which were summarized using the R package OptM v0.1.6 (Fitak 2021; available at https://rfitak.shinyapps.io/OptM/). The value of *m* that explained most of the variation in the data was determined by the Evanno method (Evanno et al. 2005), which compares the average increase in explained variance with each added migration event.

2.8. Introgression

We further wanted to evaluate whether that diversification within the *Ameivula ocellifera* complex (outgroups excluded) can be explained by a tree-like process rather than through hybridization. For this, we used the *threepop* and *fourpop* tests implemented in TreeMix (Reich et al. 2009). The *threepop* analysis tests the null hypothesis that the relationship within all possible triplets can be explained by a simple bifurcating tree with a common ancestor. A significantly negative value of the f_3-statistic suggests the presence of admixture within the triplet, and that a bifurcating tree cannot explain their relationship. Similarly, the *fourpop* analysis tests the null hypothesis that two pairs of populations can only be connected by one internal branch (e.g., the treeness of quartets). An f_4-statistic that significantly deviates from zero suggests the presence of admixture within the quartet. We also modeled uncertainty in the sample covariance matrix by implementing block jackknife resampling (−k flag) across groups of 100 unlinked SNPs.

The use of jackknife standard errors for confidence interval estimation assumes that the underlying data is normally distributed, which is often not the case with more divergent species-level allele frequency data (Meyer et al. 2017). To overcome this issue, we used the F4 python script (Meyer et al. 2017; available at https://github.com/mmatschiner/F4) to evaluate how often the observed f_4-statistic (if equal or close to zero) can be reproduced based on ILS alone (i.e., without introgression). F4 software calculates the f_4-statistic from allele frequencies of four populations and uses the coalescent-based software fastsimcoal2 (Excoffier et al. 2013) to simulate SNP data sets that mirrors the actual SNP data set, but with migration rates set to zero. A total of 10,000 coalescent simulations were carried out after a burn-in phase. Sequence data was simulated separately for all loci included in each of the four species relationships schemes. We used the same 1,308 loci dataset implemented in TreeMix and *threepop/fourpop* analysis and tested for all four-population combinations considering the four species of the *Ameivula ocellifera* complex only. We interpreted the observed f_4-statistic as evidence for introgression if less than 5 % of the 10,000 data sets simulated without introgression produced f_4 values at least as extreme as the observed.

2.9. Divergence dating

To estimate the divergence times based on UCE data among all *Ameivula* species, we used SNAPP as implemented in BEAST2. Similar to the BFD analysis, we filtered our SNP data for completeness so that there is no missing loci for any given species. For this analysis, a total of 459 biallelic SNPs without any missing data were retained in variant call format (VCF). We used the Ruby script "snapp_prep.rb" (https://github.com/mmatschiner/snapp_prep) to prepare the XML input file for SNAPP analyses. The input for the Ruby script requires a SNP matrix, a starting tree, species assignment information, divergence-time constraints, and the number of MCMC iterations. We used the VCF file filtered for unlinked SNPs containing 46 individuals and 459 biallelic sites, the ASTRAL topology as guide tree, species information based on delimitation analysis, and constrained the root age (e.g., most recent common ancestor to all *Ameivula* samples) based on the results of our mitogenome divergence-time analysis (lognormal prior; Mean = 7.3, SD = 0.13). To reduce computational demand, the tree topology was fixed in the SNAPP analyses (since overall topology is congruent among network and species tree analysis). Because introgression tests nor the predictive simulations with P2C2M.SNAPP fully reject an ILS model, the assumptions in MSMC are not violated and the divergence times are not expected to be biased (in the case of the *A. ocellifera* complex). The generated XML files were used for analyses with the SNAPP v1.5.2 (Bryant et al. 2012) package in BEAST2. We ran three independent SNAPP analyses with 1 x 10^6 MCMC iterations sampling every 1,000 steps, discarding the first 10 % of each MCMC chain as burn-in. Stationarity and chain convergence were visually checked in TRACER v1.7 (ESS > 200). A maximum-clade-credibility summary tree was generated with TreeAnnotator (BEAST2 package) and visualized in FigTree v1.4.4 (https://tree.bio.ed.ac.uk/software/figtree/).

2.10. Species network coalescent simulations and admixture proportions estimation

Both SNAPP and SNaQ analyses were based solely on autosomal data and represent the predominant genomic signal. To integrate the mtDNA information and test for mtDNA capture, we developed a topology-based approximate Bayesian computation approach. Our goals were two-fold: (i) first we wanted to evaluate what is the probability of the SNAPP species tree (bifurcating model) in generating our observed mtDNA topology versus the SNaQ phylogenetic network (network model); (ii) second, we estimated which admixture proportion maximizes the probability of observing the mtDNA topology. Mitochondrial capture would be supported if the admixture proportion required to generate our observed mtDNA tree is higher than the one estimated with our nuclear data by SNaQ. That is, the mtDNA supports a higher admixture than the autosomal data, suggesting mtDNA-cap. To that end, we used the mtDNA tree topology as rejection criterion, which differs from traditional ABC methods that use summary statistics and euclidean distance to reject simulations. Specifically, we simulated neutral data under the bifurcating and the network models, estimated by SNAPP and SNaQ respectively, and rejected the simulations that did not show at least eight of the nine samples from the species with introgressed mtDNA (MWi) as a monophyletic group with the *A. confusioniba, A. nigrigula,* and *A. xacriaba* clade. The retained simulations were used to approximate model probabilities and posterior probability distributions of admixture proportions as in a traditional ABC approach.

To simulate the species tree and network we sampled effective population sizes from a uniform distribution for each contemporary and ancestral populations/species (min: 500 K; Ne max: 2000 K). We used the topology estimated by PhyloNetworks/SNAPP (Fig. 2) as our species tree topology. To do so, we first sampled the tMRCA of all species (i.e. tree root) from a uniform distribution that reflected the credible interval estimated by SNAPP (min: 2.5 Ma; max: 9 Ma). Then, the times for the remaining nodes were sampled from a uniform distribution using the sampled root height as the upper boundary, ensuring the same node order as in the estimated species tree (min: 0.5 Ma; max: root height). To incorporate the horizontal connection in our model and simulate a network, we added a population split going backwards in time in the

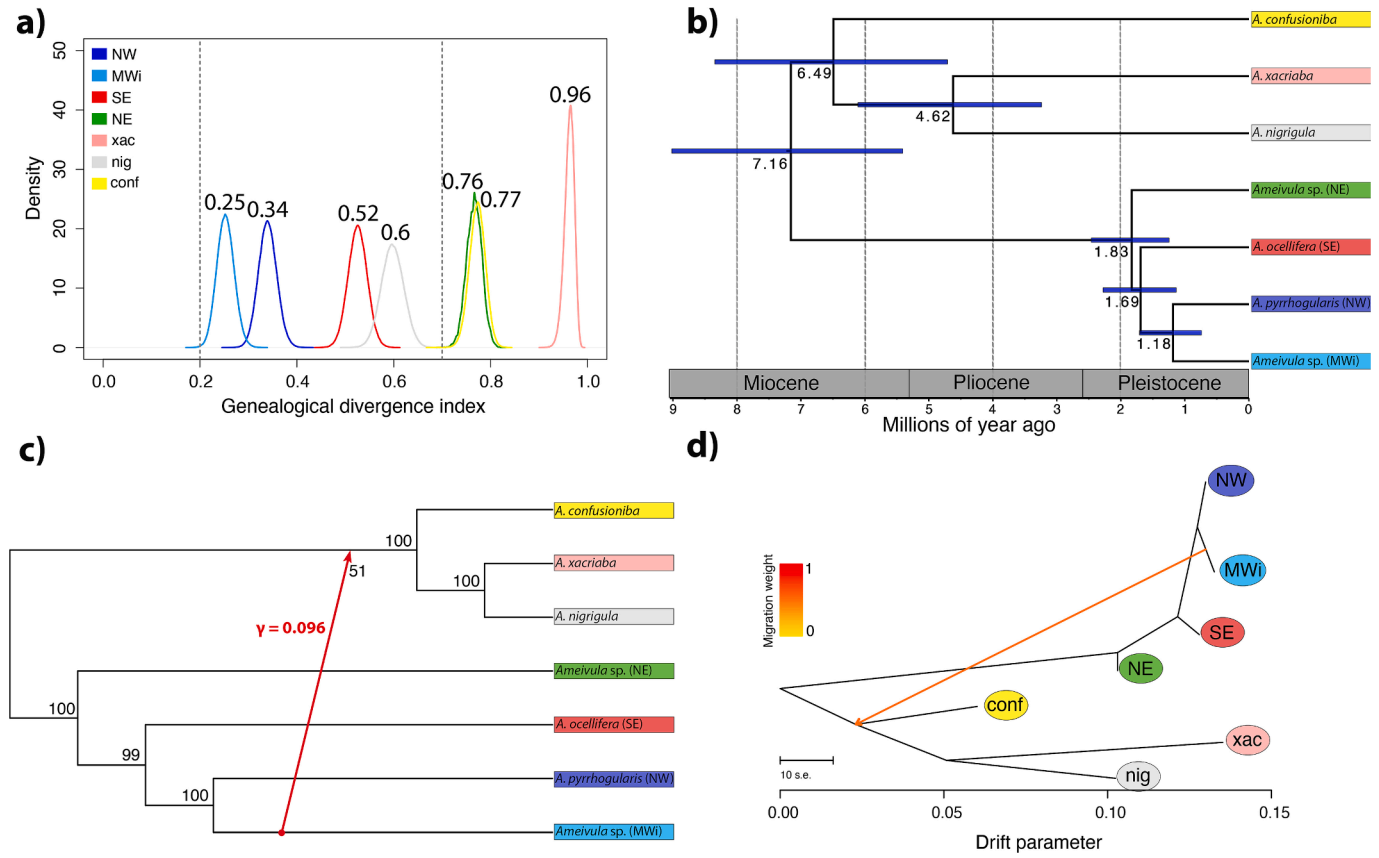

Fig. 2. a) Species delimitation applying genealogical divergence index (*gdi*). BPP was used to estimate parameters and generate density plots of *gdi* values. *gdi* < 0.2 indicates a single species, *gdi* > 0.7 indicates distinct species, and *gdi* values between 0.2 and 0.7 represent ambiguous species status (mean *gdi* values for each group are shown); b) Dated species tree inferred in SNAPP using bi-allelic SNP data. Numbers below nodes represent mean divergence times in millions of years; c) Networks analysis using SNaQ. Numbers at nodes are bootstrap support values. Value in the red arrow is percentage of introgression between lineages. Arrow direction indicates gene flow from MWi lineage into the ancestral lineage of the outgroups; and d) TreeMix results with one migration edge. The edge mixture event is colored according to the weight of the inferred edge. Arrow direction indicates gene flow from MWi lineage into the ancestral lineage of the outgroups. (For interpretation of the references to color in this figure legend, the reader is referred to the web version of this article.)

MWi species generating two ancestors (this is equivalent to a population merging forward in time, i.e. hybridization node). We forced one of these ancestors to merge with the ancestor of the three outgroup species *A. confusioniba*, *A. xacriaba,* and *A. nigrigula*, and the other ancestor to merge with the NW species, as suggested by the estimated network species tree. For the network model, the proportion of genomic contribution that each ancestor had in the genome of MWi was sampled from a uniform distribution (min: 0.01; max: 0.99). The timing of the reticulate node was sampled from a uniform distribution with a minimum of 10,000 years and an upper boundary determined by the divergence between MWi and NW. To convert sampled parameters to coalescent scale we used an average mutation rate of 1×10^{-8}. The number of individuals per population and number of base pairs of the simulated data were identical to our empirical mtDNA data.

Using the parameters described above we simulated 100 K coalescent mtDNA trees for each of the two models: (i) bifurcating species tree and (ii) species network. We then performed a rejection step on our table of 200 K simulations using a topology criterion as described above. From the retained simulations we approximated the probability of each model as their proportion in the simulation table after rejection. Using the same procedure for the species network model only, we approximated a posterior probability for the admixture proportions of each ancestral in the species with introgressed mtDNA (MWi).

2.11. Selection tests in the mtDNA

To test if the mitochondrial capture by the MWi lineage was adaptive (e.g., mitochondrial genes are evolving under a positive selection), we assessed selective footprints in the 13 mitochondrial PCG by estimating the nonsynonymous-to-synonymous substitution rate ratio (ω = dN/dS). For this analysis, we only used samples from the *Ameivula ocellifera* complex and excluded individuals with more than 10 % of missing data in the mitogenome (see Supplementary Table S1). We specified three partitions, one for each codon position. We first looked at the molecular evolution of synonymous and non-synonymous sites using robust counting with BEAST v1.10.4 (Lemey et al. 2012; Suchard et al. 2018). We ran the analysis for each gene separately and specified the codon-site-partitioned HKY model of nucleotide substitution and constant coalescent as the tree model. All other parameters were set as default. Analyses were run separately for each of the four mitochondrial lineages of the *Ameivula ocellifera* complex for 2×10^6 generations, while sampling every 200 states. We also performed a codon-based analysis using the PAML wrapper EasyCodeML v1.31 (Gao et al. 2019) to fit substitution models to the data for ω estimation using the mitogenome phylogenetic tree estimated from BEAST as input. We explicitly tested if ω can vary in different branches of the tree, selecting MWi lineage as the foreground clade (branch model). If the results were significant for the branch model, we rejected the hypothesis that all mtDNA lineages of the *A. ocellifera* complex were evolving under the same ω and further tested for diversifying selection using the branch-site models (ω can vary in different sites and branches of the tree). We also tested for positive selection among sites, where ω can vary at different sites in the gene (site model). We used the likelihood ratio test (LRT) to compare among pairs of competing models (one model was set as a null model and the second

model as the alternative model).

A summary of analysis and the goals behind each of them is summarized in Table 1 (further details can also be found in Supplementary Table S2).

3. Results

After filtering UCE loci for presence in 60 % or more of all individuals, we generated 2,560 loci of which 694 are not phylogenetically informative. We randomly sampled one SNP per locus yielding a total of 2,260 unfiltered SNPs. After filtering for non-biallelic sites and missing data, we retained 1,750 SNPs for 46 individuals for an average of 25.2 % missing data.

3.1. Mitogenome

The mitogenome pipeline recovered a maximum of 15,277 bp with an average of 13,444 bp as we successfully retrieved mtDNA information for all 50 samples. Missing data varied from 4 % to 76 % among samples, with an average of 12 % (Supplementary Table S1). The relationships inferred for the *Ameivula ocellifera* complex in our mitogenome tree was discordant with assignments from our nuclear genome data (Fig. 1a; Supplementary Tree T1). Two main clades were recognized in the mitochondrial tree: (i) one comprising samples of *A. confusioniba*, *A. nigrigula*, and *A. xacriaba*, plus individuals from the midwestern Caatinga (i.e., MWi lineage; except one individual, FRD907); and (ii) the other three species from the *A. ocellifera* complex, comprising all individuals of SE, NE, and NW plus the sample FRD907. Some clades supported by nuclear genes were not reciprocally monophyletic in the mitochondrial tree (Fig. 1a), although most interspecific relationships were strongly supported (posterior probability = 1.0, Fig. 1b, Supplementary Tree T1). For instance, only NW and *A. confusioniba* formed reciprocally monophyletic clades on both mitochondrial and concatenated UCE datasets (Fig. 1a). The mitochondrial tree confirms that MWi (supported by our delimitation analysis) had two mtDNA genomes and *A. nigrigula* was polyphyletic, with one sample more related to MWi. The same topology and relationships were inferred when the mitochondrial alignment was filtered for missing data using GBLOCK (Supplementary Tree T2). Divergence dating of the mtDNA tree suggested that the root age of all *Ameivula* samples was ~7.3 Ma (HPD: 5.9–9.1 Ma), while the *A. ocellifera* complex started to diverge around ~1.7 Ma (HPD: 1.4–2.1 Ma). Finally, the MWi clade with the introgressed mitogenome and one lineage of *A. nigrigula* from northern Bahia shared a common ancestor at ~ 2 Ma (HPD: 1.6–2.4 Ma).

3.2. Genetic structure

Both DAPC and TESS3 found similar support for three genetic clusters in the *Ameivula ocellifera* complex. These analyses also delimited the currently recognized species occurring in the Caatinga Domain and adjacent Cerrado areas (*A. confusioniba*, *A. nigrigula*, and *A. xacriaba*) in agreement with Arias et al. (2018). The DAPC analysis suggested that the best-fit K = 6 (Fig. 1b; Supplementary Fig. S1). Likewise, TESS3 validated the same clusters with K = 6, although the cross-validation criterion does not exhibit a minimum value or a plateau (Supplementary Fig. S2-3). In the TESS3 analysis considering K = 8 (Fig. 1c), the DAPC cluster from northwestern (NW) Caatinga splits into NW and midwestern (MWi), resulting in four genetic clusters in the *A. ocellifera* complex. Therefore, the southeastern lineage (hereafter SE) was structured by the São Francisco River (Fig. 1d), without any evident barriers restricting the geographic distribution of the mid-northwestern cluster (MWi and NW) and the northeastern cluster (NE). Interestingly, the MWi cluster detected by TESS3 was composed of individuals that were more closely related to the outgroup species (*A. confusioniba*, *A. nigrigula*, and *A. xacriaba*) in the mitogenome tree than to the other lineages of the *A. ocellifera* complex (Fig. 1a; more details below).

3.3. Concatenated UCE tree and species tree

The concatenated UCE tree showed good support with bootstrap values equal to 100 % for all relationships among species (Supplementary Tree T3); only the monophyletic MWi clade showed moderate

Table 1
Workflow and summary of analysis performed in this work explaining the reasoning behind each of them. SNP = single nucleotide polymorphism; MSA = multiple sequence alignment; nuc = nuclear; mt = mitochondrial. See further details in Supplementary Table S2.

Method	Data	Analysis	Goals of analysis	Main results
DAPC TESS	SNP	Population structure	Are individuals genetically structured into populations?	Analyses agreed in six genetic clusters; the MWi cluster was not found using DAPC, only in TESS with k = 8;
IQ-TREE BEAST2	MSA-nuc MSA-mt	Individual-level phylogenies	What is the phylogenetic relationships of sampled individuals? Can we recover the delimited clusters as monophyletic clades? Do nuc and mtDNA topologies agree?	Clusters are monophyletic in the nuc tree but not in the mt, with a major disagreement on the phylogenetic placement of MWi cluster (mitonuclear discordance)
BFD* *gdi*	SNP MSA-nuc	Species delimitation	Should MWi and all delimited clusters be treated as independently evolving lineages?	SE, NE, NW, and MWi are further validated with BFD*
ASTRAL SNAPP	MSA-nuc SNP	Species-level phylogeny	Does the species tree agree with the relationships inferred in the individual-level phylogenies?	Overall, it agrees with the concatenated nuclear phylogeny and places MWi within the *A. ocellifera* complex
PhyloNetworks (SNaQ) TreeMix	MSA-nuc SNP	Phylogenetic Networks/Gene flow	Can we detect the mtDNA introgression in the nuclear genome? Is their evolutionary history better explained by networks or bifurcating trees?	Analyses agreed on which species are involved in reticulation; the inferred reticulation aligns with the mtDNA introgression scenario
f-statistics	SNP	Introgression	Is gene flow occurring between species within the *Ameivula ocellifera* complex? Or is the strongest signal of gene flow between MWi and the outgroups?	Nuclear admixture can be explained by ILS, suggesting that the strongest signal of gene flow is between MWi and outgroups
SNAPP	SNP	Divergence time	When did diversification of delimited species occur? Did it happen at any specific geological period?	Divergence of the *A. ocellifera* complex dates to the early Pleistocene; last diversification occurred around 1.1Mya between MWi and NW
Topology-based ABC	Topology	Coalescent simulations	Given the species tree, how often did the simulated mitogenomes match the observed mitogenome in the bifurcating or network models?	Similarly to PhyloNetworks, simulations support a network model (99 %) over bifurcating (1 %)
			What is the proportion of admixture in simulated mitogenomes that matched the observed mtDNA topology?	Mitogenomes that matched the observed mtDNA topology suggest high admixture (~80 %), supporting mt-cap process
BEAST2 EasyCodeML	MSA-mt	Selection tests	Is there evidence of positive selection in the mitogenomes of introgressed mtDNA, supporting an adaptive mt-cap process?	Mitogenome under purifying (negative) selection; positive selection in three codons of *Cytb* in MWi; Overall, no strong evidence of adaptive mt-cap

bootstrap support (87 %). The clusters found by DAPC and TESS3 and validated by the BFD analysis formed monophyletic clusters in the UCE concatenated tree (Fig. 1; Supplementary Tree T3), unlike the mitochondrial tree (see above). Specifically, *Ameivula xacriaba* and *A. nigrigula* were sister taxa while *A. confusioniba* was sister to the *A. ocellifera* complex Clade. On the ASTRAL species tree (Supplementary Tree T4), *A. confusioniba* was sister to *A. xacriaba* + *A. nigrigula*, which was sister to the *A. ocellifera* complex Clade (see also Fig. 2b). All of these relationships were supported with posterior probability of 1.0, except for the node showing SE as the sister to the clade NW + MWi (posterior probability = 0.58).

3.4. Species delimitation

Species delimitation analyses using BFD overwhelmingly supported a model of four species in *A. ocellifera* complex (Table 2): positive BF above 200 decisively favored "model A" harboring four species. Additionally, the single species model (as proposed by Oliveira et al. 2015) was the least favored species delimitation model, followed by the two species models that represented the current taxonomy (according to Arias et al. 2018). The relationships of these four species within the SNP-based species tree was well resolved (Supplementary Tree T5). The NE was the first species to diverge, followed by the SE, with the last split occurring between NW and MWi. Posterior predictive simulations in *P2C2M.SNAPP* further demonstrated that the assumptions of the MSCM used in SNAPP was a good fit for the UCE data as all three metrics used did not suggest model violation (Supplementary Table S3).

The heuristic method (*gdi*) indicates that only the NE lineage can be supported with high confidence as a distinct species among the *Ameivula ocellifera* complex (Fig. 2a; mean *gdi* = 0.77), while SE, NW, and MWi had ambiguous support (mean *gdi* = 0.52, 0.34, and 0.25, respectively). Interestingly, the species status of *A. nigrigula* was also considered ambiguous (mean *gdi* = 0.6), while *A. confusioniba* and *A. xacriaba* are supported as distinct species (*gdi* = 0.77 and 0.96, respectively). This analysis confirms that none of the delimited clusters from the *A. ocellifera* complex Clade had support so low (*gdi* $\leq$ 0.2) to be considered genetically structured populations from the same species.

3.5. Phylogenetic networks

The network approach implemented in SNaQ indicated that at least a single reticulation event occurred during the diversification of the *Ameivula ocellifera* complex (Fig. 2c). Networks estimated in SNaQ resulted in the lowest support when no reticulation was present/allowed (h = 0), whereas the highest support according to slope heuristics was found with a single reticulation event (h = 1; Supplementary Fig. S4).

Table 2
Species delimitation based on Bayes Factor species delimitation method (BFD) for four competing models using SNAPP. Model A: outgroup + four species (SE, NE, NW, MWi), based on TESS3 results; Model B: outgroup + three species (SE, NE, NW + MWi), based on DAPC results; Model C: outgroup + two species (SE + NE, NW + MWi), based on current taxonomy; and Model D: outgroup + one species (SE + NE + NW + MWi). *Ameivula confusioniba* was used as an outgroup. Values of marginal likelihood estimation (MLE) and Bayes Factor (BF) are shown to each model. Positive BF above 200 indicates decisive support in favor of model A.

Model	Species	MLE	Rank	BF
Model A: *confusioniba* + four species (SE, NE, NW and MWi)	5	−4229.669645	1	–
Model B: *confusioniba* + three species (lump NW + MWi, split SE, NE)	4	−4337.787472	2	216
Model C: *confusioniba* + two species (lump NW + MWi, lump SE + NE)	3	−4824.218913	3	1189
Model D: *confusioniba* + one species (lump NW + MWi + SE + NE)	2	−5377.925819	4	2297

This reticulation event was inferred between the MWi and the ancestor of *A. confusioniba*, *A. nigrigula*, and *A. xacriaba*, with an estimated 9.6 % of their genomic ancestry originating from MWi (Fig. 2c). Bootstrapping of SNaQ resulted in 51 % support for this hybrid edge, while all nodes were supported at 100 %. Although a single reticulation model is preferred, a second hybrid edge was inferred between *A. nigrigula* and *A. confusioniba*, with an estimated 25 % of *A. confusioniba* genomic ancestry from *A. nigrigula* (Supplementary Fig. S5). Accordingly, TreeMix supports the same migration edge (Fig. 2d), suggesting introgression between MWi and the ancestor of the outgroup Clade (*A. confusioniba*, *A. nigrigula*, and *A. xacriaba*). Adding one migration edge to the maximum likelihood tree explains > 99 % of the variation in the data set. The Evanno method suggested that the greatest change occurred after adding a single migration edge, while adding more edges does not improve the likelihood score of the model (Supplementary Fig. S6). In summary, both analyses (SNaQ and TreeMix) agreed on which species are involved in reticulations. The network analyses detects the strongest signal of introgression, which is also present in the mitochondrial genome.

3.6. Introgression

For all triplets of species, the f_3 statistic from the *threepop* analysis was not negative, therefore, suggesting no admixture between species (Supplementary Table S4). Among the three possibilities of species quartets, only one showed significant f_4 statistics (Supplementary Table S5). Coalescent simulations further confirmed that the observed non-significant f_4 statistics and z-scores can be simulated under models with migration-free parameters (assuming *p*-values below 0.05). Therefore, introgression tests suggested that current species triples probably diverged hierarchically from a common ancestral one (e.g., species are not hybrids) and that incongruences among nuclear genes within the *A. ocellifera* species complex could result from ILS alone and not by adding an additional horizontal branch to the tree. This is supported by the quartets pairs comparison (NW,MWi;SE,NE), which were mostly congruent with the species tree (see Fig. 2b-c). This further highlights that the signal of introgression is stronger between MWi and the outgroup species.

3.7. Molecular dating

The SNP-based time-calibrated tree obtained from SNAPP (Fig. 2b; Supplementary Tree T6) suggested that the initial divergence within the *Ameivula ocellifera* complex Clade occurred with NE at ~ 1.83 Ma (95 % highest posterior density [HPD]: 1.25–2.46 Ma), followed by divergence of SE at 1.69 Ma (HPD: 1.13–2.28 Ma), and most recently between NW and MWi at 1.18 Ma (HPD: 0.74–1.71 Ma). Similar to the mitochondrial divergence time estimates (see below), the timing of diversification between these species occurred during early to mid-Pleistocene, while *A. confusioniba*, *A. nigrigula*, and *A. xacriaba* diverged in the late Miocene, starting at 6.5 Ma (HPD: 4.71–8.34 Ma).

3.8. Species network coalescent simulations and admixture proportions estimation

From a total of 200 K simulations, ~1.5 % matched the topology of our observed mtDNA tree regarding the hybrid species relationship. After rejection, our topology-based ABC approach suggested a probability of 0.99 for the network model versus a 0.01 probability for the bifurcating model. From 100 K simulations of the network model, 3.1 % matched the mtDNA topology. After rejection, we obtained a posterior distribution for the admixture proportion suggesting introgression between the ancestor of *A. confusioniba*, *A. nigrigula*, and *A. xacriaba* and MWi (Fig. 3), supporting a mt-cap process.

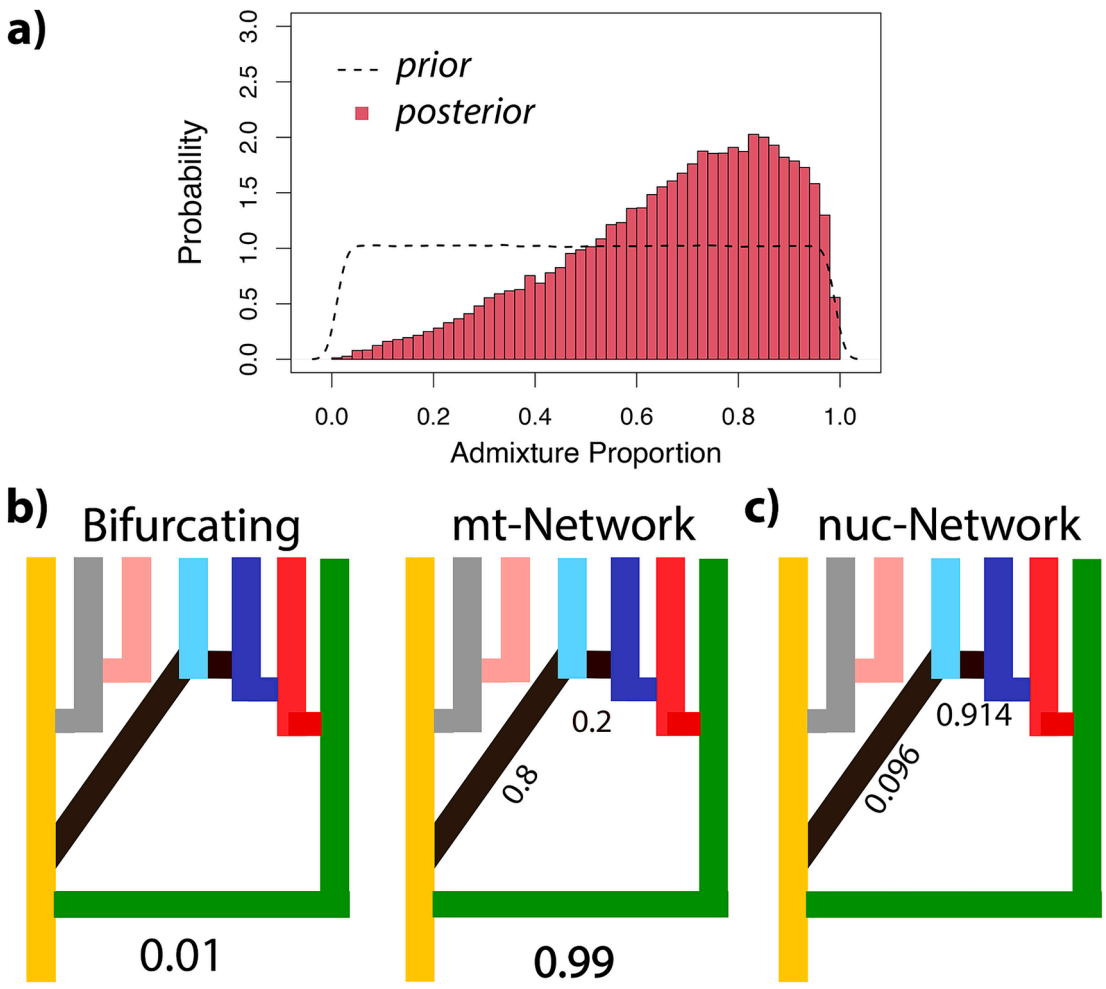

Fig. 3. a) Plots of approximated posterior probability for the admixture proportions of each ancestral in the hybrid species. b) Schematic representation of the simulated models used to assess the probability of mtDNA introgression and mean estimates of the admixture proportion supported by the mtDNA data and model probabilities as suggested by our topology-based ABC approach. c) Admixture proportion supported by nuclear data (PhyloNetworks).

3.9. Selection tests

The robust counting analysis in BEAST indicated that mitochondrial PCGs had mostly synonymous changes as fixed variants (Supplementary Table S6-7; Supplementary Fig. S7). Lineage specific dN/dS ratios estimated for mitochondrial lineages were consistent with EasyCodeML estimates (Supplementary Table S8) and ranged from 0.00117 in *COI* (Cytochrome *c* oxidase subunit 1) to 0.10873 in *ATP8* (mitochondrially encoded ATP synthase membrane subunit 8), suggesting that overall, the mtDNA genome was under strong purifying (negative) selection. Although branch models support different ω when MWi lineage was set as foreground for *Cytb* (cytochrome *b*) and *ND3* (NADH dehydrogenase subunit 3) genes, no signal of diversifying selection acting in the mtDNA lineages was detected (results not shown). Overall, tests using the branch and branch-site indicated strong purifying selection (Supplementary Table S8), although site models indicated positive selection on three amino acids encoded by *Cytb* gene (Supplementary Table S9).

4. Discussion

We used phylogenetic networks, coalescent methods, and tests of natural selection to understand the nontree-like evolution of whiptail lizards in the Caatinga Domain. Our results indicate an ancient introgression event that led to the capture of the mitochondrial genome resulting in mitonuclear genomic discordance. The mitochondrial genome data, along with species delimitation methods using genomic data, were crucial in identifying and validating MWi as an independently evolving species. The detected reticulation node, which aligns with the mtDNA introgression scenario, suggests a true biological signal rather than noise from ILS, with mtDNA suggesting higher admixture proportions than the autosomal data. We propose that MWi diversification could be due to mitonuclear incompatibilities, given the lack of geographic barriers to gene flow between MWi and other parapatric lineages and that selection in the mitogenomes is overall under purifying selection. Specifically, our results suggest that: i) specimens assigned to a widespread *Ameivula ocellifera* by Oliveira et al. (2015) are geographically structured into four species (SE, NE, NW, and MWi) without apparent geographic overlap; ii) introgression tests and posterior predictive simulations reveal a scenario of hierarchical speciation (tree-like) within the *A. ocellifera* complex, suggesting that introgressive hybridization only occurred between MWi and outgroup species; iii) divergence date estimates based on mtDNA and coalescent simulations provided insight into the timing of introgressive hybridization, suggesting that the mtDNA introgression was likely historical (during early Pleistocene) rather than ongoing; iv) the geographic displacement in nuclear and mitochondrial clades provides spatial evidence that introgression occurred at the transition zone between different climatic regimes (Caatinga and Cerrado ecotones); and v) selection tests indicate typical purifying selection occurring throughout the mitogenome of MWi but with positive selection on three amino acids encoded by *Cytb*.

4.1. Was introgression adaptive?

Our simulations strongly support a scenario of introgressive hybridization and mt-cap by MWi, with higher admixture proportions in the mtDNA (~0.8) compared to nuclear DNA (~0.09; although the direction of the introgression is not clear, see below). We identify two possible processes that can lead to higher introgression in the mitochondrial genome (Bonnet et al. 2017): (i) positive selection favoring mtDNA haplotypes in the ancestor of MWi; and (ii) admixture with selection against hybridization in the autosomal loci only, meaning neutral introgression of the mtDNA haplotypes into MWi.

Cases where the native mtDNA has been replaced by foreign ones (e.g., introduction of new variants) are likely to have some adaptive relevance (Boratyński et al. 2014; Melo-Ferreira et al. 2014; Mikkelsen and Weir 2022) and has been proposed as an important driver of speciation for many biological groups (Abbot et al. 2013), specifically for Squamate reptiles (Jančúchová-Lásková et al., 2015; Zinenko et al. 2016; Haenel and Moore, 2018; Barley et al. 2022). In lizards, for instance, positive selection on mitochondrial genes has been related to adaptation along elevation gradients (Jin et al. 2021) or efficiency on thermal regulation (Macey et al. 2021). Interestingly, MWi occurs in an area of climatic transition and elevational gradient. If adaptive introgression plays a role in the reticulate evolution identified in *Ameivula* then it is expected that loci introgressing across the genomes of MWi lineage and outgroups species (*A. confusioniba*, *A. nigrigula*, and *A. xacriaba*) should have generated unique phenotypes with associated adaptations. However, apart from the three Cytb amino acids under positive selection, we detected no signs of positive selection suggestive of an adaptive mt-cap process that would also explain the higher admixture in the mtDNA, although some adaptive relevance cannot be rejected. Therefore, we posit that selection against hybridization may be responsible for maintaining this genetic differentiation, mediated by mitonuclear incompatibilities.

It is known that poor compatibility between mtDNA and N-mtDNA genes (nuclear subunits that function in the mitochondria) can adversely affect transcription and translation of mtDNA genes into proteins, reducing individual fitness (Das 2006; Ellison and Burton 2008; Burton and Barreto 2012). For instance, previous studies showed that asexual hybrid *Aspidoscelis* lizards have reduced endurance capacity, mitochondrial respiration, and phenotypic variability in comparison to sexual species (Cullum 1996; Klabacka et al. 2022). Additionally, mitonuclear incompatibilities further induce hybrid infertility, which can drive reproductive barriers and speciation. It is worth noting that mt-cap occurred with some introgression in nuclear genes (~9%), raising the possibility that coadapted genes could have been transferred along introgressive hybridization (e.g., Beck et al. 2015; Morales et al. 2018). Mitonuclear co-introgression occurs to maintain interactions suitable for metabolic functioning (Morales et al. 2018; Haenel and Moore 2018; Mikkelsen and Weir 2022). A more thorough investigation of mitonuclear coevolution would include nuclear loci interacting with the mitochondrial genome and its products. This could help clarify if the focus of selection lies on complex interactions with nuclear-encoded peptides (e.g., Ma et al. 2016; Baris et al. 2017; Jhuang et al. 2017; Morales et al. 2018), supporting the hypothesis that mitonuclear coevolution is under play. Although at this time we cannot conclude which process is behind the mt-cap found and the differences in introgression rates between genomes, our results support that the mtDNA and the nuclear DNA of MWi evolved under different processes.

4.2. Species delimitation and status of MWi cluster

Mitonuclear interactions have been identified as an important source of reproductive barriers in numerous and diverse eukaryotic lineages (Hill 2016). Although mtDNA comprises only a tiny component of an organism's genetic material (typically $\ll$0.01 %), several features of mtDNA, such as its effect on physiology and fitness due to its metabolic role, high mutation rates, uniparental inheritance, and reduced effective population size, may lead to a disproportionate influence on hybrid incompatibilities (Sloan et al. 2017) and, ultimately, reproductive isolation (Burton and Barreto 2012; Hill 2016; 2019). Such features have led authors to propose compensatory mitonuclear coevolution as a prediction to support a speciation hypothesis, also known as the "mitonuclear compatibility species concept"; species can be recognized by a unique coadaptation of their mitochondrial and nuclear genes (Hill 2016). By adopting this theoretical framework, along with statistical support by our species delimitation analysis, we advocate for the recognition of the MWi cluster as an independently evolving species, even though it possesses two distinct mtDNA haplogroups. However, because *gdi* results were not conclusive, we suggest that additional information beyond this genetic dataset (e.g., morphology, ecophysiology) is needed to assess the species status of all delimited clusters. Interestingly, previous taxonomic studies (Silva and Ávila-Pires 2013) indicated the existence of phenotypic differences in size, coloration patterns, and hemipenis morphology between *A. pyrrhogularis* (our NW lineage) and specimens from southern Piauí State (identified by them as *Ameivula* sp.). This matches the geographic distribution of our sampled individuals from MWi, suggesting phenotypic evidence of the species status.

Processes of divergence driven by mt-cap may imply negative epistatic interactions with N-mtDNA genes during hybridization, although the remaining genomic background of diverging lineages could still be adapted to shared environmental constraints and does not reflect divergence retrieved from mtDNA (Morales et al. 2018; Bernardo et al. 2019). In such cases, shared alleles can cause deviations from species-level monophyly making species delimitation using those markers difficult. However, it is expected that ancient hybridizations and mt-cap, followed by reproductive isolation, result in the establishment of new clade-specific mutations (Hill 2016; Sloan et al. 2017). We would anticipate that according to lineage's divergence time (early to mid-Pleistocene), there would be enough accumulated clade-specific mutations to identify NW and MWi as distinct clusters. For instance, Barley et al. (2022) predicted that the timing of the hybridization event was important to define species among whiptail lizards of genus *Aspidoscelis*, with introgression events occurring during Pleistocene among diverging species. The overall shallow differentiation in the nuclear genome between MWi and NW lineages (despite deep mitogenome divergences) could be due to selection acting to maintain mitonuclear compatibilities or simply a limitation of low divergence of UCE loci. Hence, population assignment methods may have failed to discover these distinct species due to gene flow or shared polymorphism on most genes. This is because only a few genes would be under strong selection and retain the signal of divergence, thus leading to erroneous evolutionary interpretations if reticulation was undetected.

The direction of the inferred reticulation by PhyloNetworks, however, presents a significant inferential problem. According to our divergence time estimates, the origin of MWi (~1.2 Ma) occurred long after the most recent common ancestor of *A. confusioniba*, *A. nigrigula*, and *A. xacriaba* (~6.5 Ma), making it impossible for them to have exchanged genes with that ancestor at that time. A plausible explanation for this discrepancy is that only one hybridizing edge is preferred in PhyloNetworks although multiple instances of hybridization may have occurred among MWi and each extant member of the outgroup. Because the geographic ranges of MWi, *A. confusioniba* and *A. nigrigula* are currently adjacent with some overlap, past gene flow among these three taxa is feasible. Moreover, constraints in the phylogenetic relationships among the outgroup taxa can also be affecting the placement and direction of the reticulation node, since *A. xacriaba* does not occur closely to MWi but is strongly supported as sister to *A. nigrigula*. Therefore, PhyloNetworks may have oversimplified a complex evolutionary scenario, interpreting past gene flow dynamics as a single reticulation event. Resolving this analytical issue is beyond the scope of this paper. Instead, we demonstrate that while reticulations can indeed represent

true biological events of introgression, caution is necessary when interpreting reticulations showing temporal and directional inconsistencies.

4.3. Geography of introgression

The intensification of climatic oscillations in the Pleistocene may have contributed to shifting distributions of species along the tropics (Hewitt 2000), providing opportunities for secondary contact and hybridization. In the Caatinga, the effects of Pleistocene climatic fluctuations have been associated with community-level synchronous range expansion in response to vegetation shifts (Gehara et al. 2017). These expansions are likely influenced by oscillating wet and dry cycles (Auler et al. 2004; Wang et al. 2004). Accordingly, our inferences suggest that reticulation among MWi and the sampled outgroup species occurred during a time of expansion of arid vegetation and change in the landscape of Caatinga (Werneck 2011). Such changes may have facilitated population and range expansions and, consequently, hybridization. However, we have limited information on the geographic range and genomic sampling of outgroup species involved in the reticulation event, precluding us from evaluating demographic scenarios. Understanding demographic processes among species involved in the reticulation will be fundamental to better understanding the rate and direction of introgression (Currat et al. 2008) given that it is expected that introgressive hybridization occurs during populational range shifts (Melo-Ferreira et al. 2012; Marques et al. 2017). Finally, we showed that the mitochondrial genome of the MWi lineage was not completely replaced by this introgression event; one individual of the MWi lineage is related as a sister of the NW lineage.

According to the displacement in geographic distribution of the *Ameivula ocellifera* complex defined by mtDNA and nuDNA genomes, the northern Bahia-southern Piauí region is where introgression likely occurred. This region is characterized as transitional between the Caatinga and Cerrado vegetation and has already been identified as an area of high nucleotide and haplotype diversity for vertebrates and invertebrates along the Caatinga (Oliveira et al. 2015; Oliveira et al. 2018; Fonseca et al. 2019). It is also the center of initial dispersal for the *Ameivula ocellifera* complex diversification (Oliveira et al. 2015). This area includes several endemic species with significant population structure (e.g., Lanna et al. 2018; Recoder and Rodrigues 2020), suggesting that the region may have acted as a refugium in periods of lineage isolation promoted by the climatic changes of the Pleistocene when capture took place. A thorough study of the contact zones and more information on the ecology, physiology, reproductive behavior, and evolutionary niches of these lizards may be necessary to understand conditions facilitating introgression.

4.4. Taxonomic implications

Our UCE data supports strong genetic structure within the Caatinga, rejecting the previous taxonomic hypotheses proposed by both Oliveira et al. (2015) and Arias et al. (2018). The taxonomic decisions made by those authors are justifiable given their results but were limited by the number and types of markers and analysis that could not account for the presence of historical introgressive hybridization. These limitations are known to generate conflicting or ambiguous species delimitation (Grummer et al. 2014; Chan et al. 2021). For instance, it is very likely that Arias et al. (2018) may have inadvertently relied on the phylogenetic placement of individuals with introgressed mtDNA to revalidate *A. pyrrhogularis* (our NW cluster) since their vouchers are from localities within MWi geographic range and, likewise, do not cluster within the *A. ocellifera* complex. We have a better-informed species delimitation result by using a comprehensive genomic dataset appropriately testing for reticulate evolution, and implementing model-based species delimitation methods that explicitly test for competing species sets without relying solely on topology (e.g., phylogenetic placement) or mtDNA divergence. We further suggest a reassessment of phenotypic variation applied to distinguish *Ameivula* species to agree with molecular data, as it has been previously implied that morphology data support additional species beyond the currently recognized *A. ocellifera* and *A. pyrrhogularis* (see Silva and Ávila-Pires 2013; Arias et al. 2018). We also encourage future research to evaluate these species physiological traits, assuming that introgression should have generated unique adaptations (e.g., Cullum 1996; Klabacka et al. 2022).

Given that deep time reticulation and contemporary introgression seem common in several lizard species worldwide (Burbrink and Ruane 2021), we also suggest that these events should be examined in future studies of *Ameivula* relationships. For instance, in a related teiid taxa of genus *Aspidoscelis*, diversification is marked in many instances by recurrent hybridization (Barley et al. 2019; 2022). Similarly, the diversification of Andean species of the iguanian genus *Liolemus* is marked by extensive reticulation related to introgressive hybridization during rapid radiation events and colonization of new habitats (Grummer et al. 2021; Esquerré et al. 2022). Here, we report for the first time that reticulate evolution also occurs among squamate taxa along seasonally dry tropical forests in South America. Therefore, using mitochondria and few nuclear loci as the main source of taxonomic decision making for the group may be unreliable. Our results highlight the importance of investigating introgressive hybridization, non-treelike diversification, and selection when mitonuclear incongruencies are detected.

5. Conclusions

Despite genomic data providing a more refined resolution in terms of genetic structure, it is important to investigate the evolution of the mitochondrial and nuclear genomes to understand the speciation process and have better-informed species delimitation. Phylogenomic approaches have led to increased resolution in many taxonomic groups, especially when combined with explicit tests of complex or non-treelike evolutionary processes. By using genome-wide data with phylogenetic network analyses and mitochondrial tree simulations, we demonstrated that the evolutionary history of *Ameivula* species inhabiting the Caatinga Domain is complex and characterized by at least one ancient reticulation event, which resulted on the interspecific capture of the mitogenome. We further highlight that by using UCE data alone, the recognition of these species and the processes behind mitonuclear incongruences would not be completely understood. For instance, the network analyses seem to detect the strong signal of introgression. The inferred single reticulation node aligns with the mtDNA introgression scenario, indicating it could reflect a real biological signal rather than noise from ILS. These findings will be pivotal for future work on neotropical lizards including other *Ameivula* species. Much of the *Ameivula* range is poorly sampled and future surveys of currently unsampled populations may lead to recognition of additional species and stronger support for the role of reticulate evolution in the diversification of this group.

CRediT authorship contribution statement

Felipe de M. Magalhães: Conceptualization, Methodology, Software, Formal analysis, Investigation, Data curation, Writing – original draft, Writing – review & editing.. **Eliana F. Oliveira:** Writing – review & editing, Visualization, Data curation. **Adrian A. Garda:** Writing – review & editing, Visualization, Resources. **Frank T. Burbrink:** Writing – review & editing, Visualization, Resources, Funding acquisition, Data curation. **Marcelo Gehara:** Writing – review & editing, Writing – original draft, Visualization, Validation, Supervision, Software, Methodology, Investigation, Formal analysis, Data curation, Conceptualization.

Funding

This study was funded from two National Science Foundation grants

grants to FTB: Dimensions USBIOTA 1831241 and NSF-DEB 2323125.

Declaration of Competing Interest

The authors declare that they have no known competing financial interests or personal relationships that could have appeared to influence the work reported in this paper.

Acknowledgments

FMM thanks Wilson Guillory and Ricardo da Silveira-Filho for their help with R scripts/coding. We also thank David Kizirian and Lauren Vonnahme at the AMNH for help with importing tissues. We acknowledge the two anonymous reviewers for improving the quality of the manuscript. This research was supported in part from ato NSF grants to FTB: Dimensions USBIOTA 1831241 and NSF_DEB-2323125. EFO thanks Conselho Nacional de Desenvolvimento Científico e Tecnológico (CNPq) and Fundação de Apoio ao Desenvolvimento do Ensino, Ciência e Tecnologia do Estado de Mato Grosso do Sul (FUNDECT) for her post-doctoral fellowships (FUNDECT/CNPq/SECTEI N°19/2015–DCR and FUNDECT 32/2021). MG thanks his family and his diatonic accordion for creating compelling opportunities for breaks from work. AAG thanks CNPq for support in the form of grants and productivity scholarship (406968/2021-7, 307643/2022-0).

Appendix A. Supplementary data

Supplementary data to this article can be found online at https://doi.org/10.1016/j.ympev.2024.108280.

Data availability

I have shared supplementary data on the attach file step

References

Abbott, R., Albach, D., Ansell, S., Arntzen, J.W., Baird, S.J., Bierne, N., Boughman, J., Brelsford, A., Buerkle, C.A., Buggs, R., Butlin, R.K., Dieckmann, U., Eroukhmanoff, F., Grill, A., Cahan, S.H., Hermansen, J.S., Hewitt, G., Hudson, A.G., Jiggins, C., Jones, J., Keller, B., Marczewski, T., Mallet, J., Martinez-Rodriguez, P., Most, M., Mullen, S., Nichols, R., Nolte, A.W., Parisod, C., Pfennig, K., Rice, A.M., Ritchie, M.G., Seifert, B., Smadja, C.M., Stelkens, R., Szymura, J.M., Vainola, R., Wolf, J.B., Zinner, D., 2013. Hybridization and speciation. J. Evol. Biol. 26, 229–246. https://doi.org/10.1111/j.1420-9101.2012.02599.x.

Andrew, R.L., Rieseberg, L.H., 2013. Divergence is focused on few genomic regions early in speciation: incipient speciation of sunflower ecotypes. Evolution 67, 2468–2482. https://doi.org/10.1111/evo.12106.

Ané, C., Larget, B., Baum, D.A., Smith, S.D., Rokas, A., 2007. Bayesian estimation of concordance among gene trees. Mol. Biol. Evol. 24, 412–426. https://doi.org/10.1093/molbev/msl170.

Arias, F.J., Recoder, R., Álvarez, B.B., Ethcepare, E., Quipildor, M., Lobo, F., Rodrigues, M.T., 2018. Diversity of teiid lizards from Gran Chaco and western Cerrado (Squamata: Teiidae). Zool. Scr. 47, 144–158. https://doi.org/10.1111/zsc.12277.

Auler, A.S., Wang, X., Edwards, R.L., Cheng, H., Cristalli, P.S., Smart, P.L., Richards, D. A., 2004. Quaternary ecological and geomorphic changes associated with rainfall events in presently semi-arid northeastern Brazil. J. Quat. Sci. 19, 693–701. https://doi.org/10.1002/jqs.876.

Ballard, J.W., Whitlock, M.C., 2004. The incomplete natural history of mitochondria. Mol. Ecol. 13, 729–744. https://doi.org/10.1046/j.1365-294X.2003.02063.x.

Baris, T.Z., Wagner, D.N., Dayan, D.I., Du, X., Blier, P.U., Pichaud, N., Oleksiak, M.F., Crawford, D.L., 2017. Evolved genetic and phenotypic differences due to mitochondrial-nuclear interactions. PLoS Genet. 13, e1006517. https://doi.org/10.1371/journal.pgen.1006517.

Barley, A.J., Nieto-Montes de Oca, A., Reeder, T.W., Manriquez-Moran, N.L., Arenas Monroy, J.C., Hernández-Gallegos, O., Thomson, R.C., 2019. Complex patterns of hybridization and introgression across evolutionary timescales in Mexican whiptail lizards (*Aspidoscelis*). Mol. Phylogenet. Evol. 132, 284–295. https://doi.org/10.1016/j.ympev.2018.12.016.

Barley, A.J., de Oca, A.N., Manríquez-Morán, N.L., Thomson, R.C., 2022. The evolutionary network of whiptail lizards reveals predictable outcomes of hybridization. Science 377, 773–777. https://doi.org/10.1126/science.abn1593.

Bar-Yaacov, D., Blumberg, A., Mishmar, D., 2012. Mitochondrial-nuclear co-evolution and its effects on OXPHOS activity and regulation. BBA 1819, 1107–1111. https://doi.org/10.1016/j.bbagrm.2011.10.008.

Bar-Yaacov, D., Hadjivasiliou, Z., Levin, L., Barshad, G., Zarivach, R., Bouskila, A., Mishmar, D., 2015. Mitochondrial involvement in vertebrate speciation? the case of mito-nuclear genetic divergence in chameleons. Genome Biol. Evol. 7, 3322–3336. https://doi.org/10.1093/gbe/evv226.

Beck, E.A., Thompson, A.C., Sharbrough, J., Brud, E., Llopart, A., 2015. Gene flow between *Drosophila yakuba* and *Drosophila santomea* in subunit V of cytochrome c oxidase: A potential case of cytonuclear cointrogression. Evolution 69, 1973–1986. https://doi.org/10.1111/evo.12718.

Bernardo, P.H., Sanchez-Ramirez, S., Sanchez-Pacheco, S.J., Alvarez-Castaneda, S.T., Aguilera-Miller, E.F., Mendez-de la Cruz, F.R., Murphy, R.W., 2019. Extreme mito-nuclear discordance in a peninsular lizard: the role of drift, selection, and climate. Heredity 123, 359–370. https://doi.org/10.1038/s41437-019-0204-4.

Bonnet, T., Leblois, R., Rousset, F., Crochet, P.A., 2017. A reassessment of explanations for discordant introgressions of mitochondrial and nuclear genomes. Evolution 71, 2140–2158. https://doi.org/10.1111/evo.13296.

Boratyński, Z., Melo-Ferreira, J., Alves, P.C., Berto, S., Koskela, E., Pentikäinen, O.T., Tarroso, P., Ylilauri, M., Mappes, T., 2014. Molecular and ecological signs of mitochondrial adaptation: consequences for introgression? Heredity 113, 277–286. https://doi.org/10.1038/hdy.2014.28.

Bouckaert, R.R., Drummond, A.J., 2017. bModelTest: Bayesian phylogenetic site model averaging and model comparison. BMC Evol. Biol. 17, 42. https://doi.org/10.1186/s12862-017-0890-6.

Bouckaert, R., Heled, J., Kuhnert, D., Vaughan, T., Wu, C.H., Xie, D., Suchard, M.A., Rambaut, A., Drummond, A.J., 2014. BEAST 2: a software platform for Bayesian evolutionary analysis. PLoS Comput. Biol. 10, e1003537. https://doi.org/10.1371/journal.pcbi.1003537.

Breton, S., Milani, L., Ghiselli, F., Guerra, D., Stewart, D.T., Passamonti, M., 2014. A resourceful genome: updating the functional repertoire and evolutionary role of animal mitochondrial DNAs. Trends Genet. 30, 555–564. https://doi.org/10.1016/j.tig.2014.09.002.

Bryant, D., Bouckaert, R., Felsenstein, J., Rosenberg, N.A., RoyChoudhury, A., 2012. Inferring species trees directly from biallelic genetic markers: bypassing gene trees in a full coalescent analysis. Mol. Biol. Evol. 29, 1917–1932. https://doi.org/10.1093/molbev/mss086.

Burbrink, F.T., Gehara, M., 2018. The biogeography of deep time phylogenetic reticulation. Syst. Biol. 67, 743–744. https://doi.org/10.1093/sysbio/syy019.

Burbrink, F.T., Grazziotin, F.G., Pyron, R.A., Cundall, D., Donnellan, S., Irish, F., Keogh, J.S., Kraus, F., Murphy, R.W., Noonan, B., Raxworthy, C.J., Ruane, S., Lemmon, A.R., Lemmon, E.M., Zaher, H., 2020. Interrogating genomic-scale data for Squamata (lizards, snakes, and amphisbaenians) shows no support for key traditional morphological relationships. Syst. Biol. 69, 502–520. https://doi.org/10.1093/sysbio/syz062.

Burbrink, F.T., Ruane, S., 2021. Contemporary philosophy and methods for studying speciation and delimiting species. Ichthyol. Herpetol. 109, 874–894. https://doi.org/10.1643/h2020073.

Burbrink, F.T., Gehara, M., Myers, E.A., 2021. Resolving spatial complexities of hybridization in the context of the gray zone of speciation in North American ratsnakes (*Pantherophis obsoletus* complex). Evolution 75, 260–277. https://doi.org/10.1111/evo.14141.

Burton, R.S., Barreto, F.S., 2012. A disproportionate role for mtDNA in Dobzhansky-Muller incompatibilities? Mol. Ecol. 21, 4942–4957. https://doi.org/10.1111/mec.12006.

Cahill, J.A., Heintzman, P.D., Harris, K., Teasdale, M.D., Kapp, J., Soares, A.E.R., Stirling, I., Bradley, D., Edwards, C.J., Graim, K., Kisleika, A.A., Malev, A.V., Monaghan, N., Green, R.E., Shapiro, B., 2018. Genomic evidence of widespread admixture from polar bears into brown bears during the last ice age. Mol. Biol. Evol. 35, 1120–1129. https://doi.org/10.1093/molbev/msy018.

Cairns, N.A., Cicchino, A.S., Stewart, K.A., Austin, J.D., Lougheed, S.C., 2021. Cytonuclear discordance, reticulation and cryptic diversity in one of North America's most common frogs. Mol. Phylogenet. Evol. 156, 107042. https://doi.org/10.1016/j.ympev.2020.107042.

Castellana, S., Vicario, S., Saccone, C., 2011. Evolutionary patterns of the mitochondrial genome in Metazoa: exploring the role of mutation and selection in mitochondrial protein coding genes. Genome Biol. Evol. 3, 1067–1079. https://doi.org/10.1093/gbe/evr040.

Castresana, J., 2000. Selection of conserved blocks from multiple alignments for their use in phylogenetic analysis. Mol. Biol. Evol. 17, 540–542. https://doi.org/10.1093/oxfordjournals.molbev.a026334.

Caye, K., Jay, F., Michel, O., François, O., 2018. Fast inference of individual admixture coefficients using geographic data. Ann. Appl. Stat. 12, 586–608. https://doi.org/10.1214/17-AOAS1106.

Chan, K.O., Hutter, C.R., Wood, P.L., Su, Y.C., Brown, R.M., 2021. Gene flow increases phylogenetic structure and inflates cryptic species estimations: a case study on widespread Philippine puddle frogs (*Occidozyga laevis*). Syst. Biol. 71, 40–57. https://doi.org/10.1093/sysbio/syab034.

Cullum, A.J., 1996. Comparisons of physiological performance in sexual and asexual whiptail lizards (Genus *Cnemidophorus*): implications for the role of heterozygosity. Am. Nat. 150, 24–47. https://doi.org/10.1086/286055.

Currat, M., Ruedi, M., Petit, R.J., Excoffier, L., 2008. The hidden side of invasions: massive introgression by local genes. Evolution 62, 1908–1920. https://doi.org/10.1111/j.1558-5646.2008.00413.x.

da Fonseca, R.R., Johnson, W.E., O'Brien, S.J., Ramos, M.J., Antunes, A., 2008. The adaptive evolution of the mammalian mitochondrial genome. BMC Genomics 9, 119. https://doi.org/10.1186/1471-2164-9-119.

Danecek P., Bonfield J.K., Liddle J., Marshall J., Ohan V., Pollard M.O., Whitwham A., Keane T., McCarthy S.A., Davies R.M., Li H. 2021. Twelve years of SAMtools and BCFtools. Gigascience 10:giab008. https://doi.org/10.1093/gigascience/giab008.
Das, J., 2006. The role of mitochondrial respiration in physiological and evolutionary adaptation. Bioessays 28, 890–901. https://doi.org/10.1002/bies.20463.
de Queiroz, K., 2007. Species concepts and species delimitation. Syst. Biol. 56, 879–886. https://doi.org/10.1080/10635150701701083.
Dinca, V., Lee, K.M., Vila, R., Mutanen, M., 2019. The conundrum of species delimitation: a genomic perspective on a mitogenetically super-variable butterfly. Proc. Biol. Sci. 286, 20191311. https://doi.org/10.1098/rspb.2019.1311.
Duckett, D.J., Pelletier, T.A., Carstens, B.C., 2020. Identifying model violations under the multispecies coalescent model using P2C2M.SNAPP. PeerJ 8 (e8271). https://doi.org/10.7717/peerj.8271.
Ellison, C.K., Burton, R.S., 2008. Interpopulation hybrid breakdown maps to the mitochondrial genome. Evolution 62, 631–638. https://doi.org/10.1111/j.1558-5646.2007.00305.x.
Esquerré, D., Keogh, J.S., Demangel, D., Morando, M., Avila, L.J., Sites, J.W., Ferri-Yanez, F., Leaché, A.D., 2022. Rapid radiation and rampant reticulation: phylogenomics of South American *Liolaemus* lizards. Syst. Biol. 71, 286–300. https://doi.org/10.1093/sysbio/syab058.
Evanno, G., Regnaut, S., Goudet, J., 2005. Detecting the number of clusters of individuals using the software STRUCTURE: a simulation study. Mol. Ecol. 14, 2611–2620. https://doi.org/10.1111/j.1365-294X.2005.02553.x.
Excoffier, L., Dupanloup, I., Huerta-Sanchez, E., Sousa, V.C., Foll, M., 2013. Robust demographic inference from genomic and SNP data. PLoS Genet. 9, e1003905. https://doi.org/10.1371/journal.pgen.1003905.
Faircloth, B.C., 2016. PHYLUCE is a software package for the analysis of conserved genomic loci. Bioinformatics 32, 786–788. https://doi.org/10.1093/bioinformatics/btv646.
Faircloth, B.C., McCormack, J.E., Crawford, N.G., Harvey, M.G., Brumfield, R.T., Glenn, T.C., 2012. Ultraconserved elements anchor thousands of genetic markers spanning multiple evolutionary timescales. Syst. Biol. 61, 717–726. https://doi.org/10.1093/sysbio/sys004.
Fitak, R.R., 2021. OptM: estimating the optimal number of migration edges on population trees using Treemix. Biol. Methods Protoc. 6 (bpab017). https://doi.org/10.1093/biomethods/bpab017.
Flouri, T., Jiao, X., Rannala, B., Yang, Z., 2018. Species tree inference with BPP using genomic sequences and the multispecies coalescent. Mol. Biol. Evol. 35, 2585–2593. https://doi.org/10.1093/molbev/msy147.
Fonseca, E.M., Werneck, F.P., Gehara, M., Oliveira, E.F., Magalhães, F.d.M., Lanna, F.M., Lima, G.S., Marques, R., Mesquita, D.O., Costa, G.C., Colli, G.R., Garda, A.A., 2019. The role of strict nature reserves in protecting genetic diversity in a semiarid vegetation in Brazil. Biodivers. Conserv. 28, 2877–2890. https://doi.org/10.1007/s10531-019-01802-y.
Gao, F., Chen, C., Arab, D.A., Du, Z., He, Y., Ho, S.Y.W., 2019. EasyCodeML: A visual tool for analysis of selection using CodeML. Ecol. Evol. 9, 3891–3898. https://doi.org/10.1002/ece3.5015.
Gehara, M., Garda, A.A., Werneck, F.P., Oliveira, E.F., da Fonseca, E.M., Camurugi, F., Magalhaes, F.M., Lanna, F.M., Sites Jr., J.W., Marques, R., Silveira-Filho, R., Sao Pedro, V.A., Colli, G.R., Costa, G.C., Burbrink, F.T., 2017. Estimating synchronous demographic changes across populations using hABC and its application for a herpetological community from northeastern Brazil. Mol. Ecol. 26, 4756–4771. https://doi.org/10.1111/mec.14239.
Gershoni, M., Templeton, A.R., Mishmar, D., 2009. Mitochondrial bioenergetics as a major motive force of speciation. Bioessays 31, 642–650. https://doi.org/10.1002/bies.200800139.
Gruber, B., Unmack, P.J., Berry, O.F., Georges, A., 2018. dartr: An r package to facilitate analysis of SNP data generated from reduced representation genome sequencing. Mol. Ecol. Resour. 18, 691–699. https://doi.org/10.1111/1755-0998.12745.
Grummer, J.A., Bryson Jr., R.W., Reeder, T.W., 2014. Species delimitation using bayes factors: simulations and application to the *Sceloporus scalaris* species group (Squamata: Phrynosomatidae). Syst. Biol. 63, 119–133. https://doi.org/10.1093/sysbio/syt069.
Grummer, J.A., Avila, L.J., Morando, M.M., Leaché, A.D., 2021. Four species linked by three hybrid zones: two instances of repeated hybridization in one species group (Genus *Liolaemus*). Front. Ecol. Evol. 9, 624109. https://doi.org/10.3389/fevo.2021.624109.
Haenel, G.J., Moore, V.D.G., 2018. Functional divergence of mitochondria and coevolution of genomes: cool mitochondria in hot lizards. Physiol. Biochem. Zool. 91, 1068–1081. https://doi.org/10.1086/699918.
Harrison, R.G., Larson, E.L., 2014. Hybridization, introgression, and the nature of species boundaries. J. Hered. 105 (Suppl 1), 795–809. https://doi.org/10.1093/jhered/esu033.
Harvey, M.G., Smith, B.T., Glenn, T.C., Faircloth, B.C., Brumfield, R.T., 2016. Sequence capture versus restriction site associated DNA sequencing for shallow systematics. Syst. Biol. 65, 910–924. https://doi.org/10.1093/sysbio/syw036.
Hebert, P.D., Cywinska, A., Ball, S.L., deWaard, J.R., 2003. Biological identifications through DNA barcodes. Proc. Biol. Sci. 270, 313–321. https://doi.org/10.1098/rspb.2002.2218.
Heliconius, G.C., 2012. Butterfly genome reveals promiscuous exchange of mimicry adaptations among species. Nature 487, 94–98. https://doi.org/10.1038/nature11041.
Henault, M., Landry, C.R., 2017. When nuclear-encoded proteins and mitochondrial RNAs do not get along, species split apart. EMBO Rep. 18, 8–10. https://doi.org/10.15252/embr.201643645.
Hewitt, G., 2000. The genetic legacy of the Quaternary ice ages. Nature 405, 907–913. https://doi.org/10.1038/35016000.
Hill, G.E., 2015. Mitonuclear ecology. Mol. Biol. Evol. 32, 1917–1927. https://doi.org/10.1093/molbev/msv104.
Hill, G.E., 2016. Mitonuclear coevolution as the genesis of speciation and the mitochondrial DNA barcode gap. Ecol. Evol. 6, 5831–5842. https://doi.org/10.1002/ece3.2338.
Hill, G.E., 2019. Reconciling the mitonuclear compatibility species concept with rampant mitochondrial introgression. Integr. Comp. Biol. 59, 912–924. https://doi.org/10.1093/icb/icz019.
Jackson, N.D., Carstens, B.C., Morales, A.E., O'Meara, B.C., 2017. Species delimitation with gene flow. Syst. Biol. 66, 799–812. https://doi.org/10.1093/sysbio/syw117.
Jančúchová-Lásková, J., Landová, E., Frynta, D., 2015. Are genetically distinct lizard species able to hybridize? A review. Curr. Zool. 61, 155–180. https://doi.org/10.1093/czoolo/61.1.155.
Jhuang, H.Y., Lee, H.Y., Leu, J.Y., 2017. Mitochondrial-nuclear co-evolution leads to hybrid incompatibility through pentatricopeptide repeat proteins. EMBO Rep. 18, 87–101. https://doi.org/10.15252/embr.201643311.
Jin Y., D Y.C.B., Li J., Wo Y., Tong H., Shchur V. 2021. Elevation as a selective force on mitochondrial respiratory chain complexes of the *Phrynocephalus* lizards in the Tibetan plateau. Curr Zool 67:191–199. https://doi.org/10.1093/cz/zoaa056.
Jombart, T., 2008. adegenet: a R package for the multivariate analysis of genetic markers. Bioinformatics 24, 1403–1405. https://doi.org/10.1093/bioinformatics/btn129.
Jombart, T., Devillard, S., Balloux, F., 2010. Discriminant analysis of principal components: a new method for the analysis of genetically structured populations. BMC Genet. 11, 94. https://doi.org/10.1186/1471-2156-11-94.
Jones, M.R., Mills, L.S., Alves, P.C., Callahan, C.M., Alves, J.M., Lafferty, D.J.R., Jiggins, F.M., Jensen, J.D., Melo-Ferreira, J., Good, J.M., 2018. Adaptive introgression underlies polymorphic seasonal camouflage in snowshoe hares. Science 360, 1355–1358. https://doi.org/10.1126/science.aar5273.
Kalyaanamoorthy, S., Minh, B.Q., Wong, T.K.F., von Haeseler, A., Jermiin, L.S., 2017. ModelFinder: fast model selection for accurate phylogenetic estimates. Nat. Methods 14, 587–589. https://doi.org/10.1038/nmeth.4285.
Kass, R.E., Raftery, A.E., 1995. Bayes factor. J. Am. Stat. Assoc. 90, 773–795. https://doi.org/10.1080/01621459.1995.10476572.
Kearse, M., Moir, R., Wilson, A., Stones-Havas, S., Cheung, M., Sturrock, S., Buxton, S., Cooper, A., Markowitz, S., Duran, C., Thierer, T., Ashton, B., Meintjes, P., Drummond, A., 2012. Geneious Basic: an integrated and extendable desktop software platform for the organization and analysis of sequence data. Bioinformatics 28, 1647–1649. https://doi.org/10.1093/bioinformatics/bts199.
Klabacka, R.L., Parry, H.A., Yap, K.N., Cook, R.A., Herron, V.A., Horne, L.M., Wolak, M.E., Maldonado, J.A., Fujita, M.K., Kavazis, A.N., Oaks, J.R., Schwartz, T.S., 2022. Reduced mitochondrial respiration in hybrid asexual lizards. Am. Nat. 199, 719–728. https://doi.org/10.1086/719014.
Korneliussen, T.S., Albrechtsen, A., Nielsen, R., 2014. ANGSD: Analysis of Next Generation Sequencing Data. BMC Bioinf. 15, 356. https://doi.org/10.1186/s12859-014-0356-4.
Lamb, A.M., Gan, H.M., Greening, C., Joseph, L., Lee, Y.P., Moran-Ordonez, A., Sunnucks, P., Pavlova, A., 2018. Climate-driven mitochondrial selection: A test in Australian songbirds. Mol. Ecol. 27, 898–918. https://doi.org/10.1111/mec.14488.
Lanna, F.M., Werneck, F.P., Gehara, M., Fonseca, E.M., Colli, G.R., Sites Jr., J.W., Rodrigues, M.T., Garda, A.A., 2018. The evolutionary history of *Lygodactylus* lizards in the South American open diagonal. Mol. Phylogenet. Evol. 127, 638–645. https://doi.org/10.1016/j.ympev.2018.06.010.
Leaché, A.D., Fujita, M.K., Minin, V.N., Bouckaert, R.R., 2014. Species delimitation using genome-wide SNP data. Syst. Biol. 63, 534–542. https://doi.org/10.1093/sysbio/syu018.
Leaché, A.D., Zhu, T., Rannala, B., Yang, Z., 2019. The spectre of too many species. Syst. Biol. 68, 168–181. https://doi.org/10.1093/sysbio/syy051.
Lemey, P., Minin, V.N., Bielejec, F., Kosakovsky Pond, S.L., Suchard, M.A., 2012. A counting renaissance: combining stochastic mapping and empirical Bayes to quickly detect amino acid sites under positive selection. Bioinformatics 28, 3248–3256. https://doi.org/10.1093/bioinformatics/bts580.
Li, H., Durbin, R., 2009. Fast and accurate short read alignment with Burrows-Wheeler transform. Bioinformatics 25, 1754–1760. https://doi.org/10.1093/bioinformatics/btp324.
Ma, H., Marti, G.N., Morey, R., Van Dyken, C., Kang, E., Hayama, T., Lee, Y., Li, Y., Tippner-Hedges, R., Wolf, D.P., Laurent, L.C., Mitalipov, S., 2016. Incompatibility between nuclear and mitochondrial genomes contributes to an interspecies reproductive barrier. Cell Metab. 24, 283–294. https://doi.org/10.1016/j.cmet.2016.06.012.
Macey, J., Pabinger, S., Barbieri, C.G., Buring, E.S., Gonzalez, V.L., Mulcahy, D.G., DeMeo, D.P., Urban, L., Hime, P.M., Prost, S., Elliot, A.N., Gemmell, N.J., 2021. Evidence of two deeply divergent co-existing mitochondrial genomes in the Tuatara reveals an extremely complex genomic organization. Commun. Biol. 4, 116. https://doi.org/10.1038/s42003-020-01639-0.
Mallet, J., Besansky, N., Hahn, M.W., 2016. How reticulated are species? Bioessays 38, 140–149. https://doi.org/10.1002/bies.201500149.
Marques, J.P., Farelo, L., Vilela, J., Vanderpool, D., Alves, P.C., Good, J.M., Boursot, P., Melo-Ferreira, J., 2017. Range expansion underlies historical introgressive hybridization in the Iberian hare. Sci. Rep. 7, 40788. https://doi.org/10.1038/srep40788.
Martin, S.H., Davey, J.W., Salazar, C., Jiggins, C.D., 2019. Recombination rate variation shapes barriers to introgression across butterfly genomes. PLoS Biol. 17, e2006288. https://doi.org/10.1371/journal.pbio.2006288.

Mason, A.J., Grazziotin, F.G., Zaher, H., Lemmon, A.R., Moriarty, L.E., Parkinson, C.L., 2019. Reticulate evolution in nuclear Middle America causes discordance in the phylogeny of palm-pitvipers (Viperidae: *Bothriechis*). J. Biogeogr. 46, 833–844. https://doi.org/10.1111/jbi.13542.

Mayr, E., 1963. Animal Species and Evolution. Massachusetts, Belknap Press of Harvard University Press, Cambridge.

McGee, M.D., Borstein, S.R., Meier, J.I., Marques, D.A., Mwaiko, S., Taabu, A., Kishe, M. A., O'Meara, B., Bruggmann, R., Excoffier, L., Seehausen, O., 2020. The ecological and genomic basis of explosive adaptive radiation. Nature 586, 75–79. https://doi.org/10.1038/s41586-020-2652-7.

McKenna, A., Hanna, M., Banks, E., Sivachenko, A., Cibulskis, K., Kernytsky, A., Garimella, K., Altshuler, D., Gabriel, S., Daly, M., DePristo, M.A., 2010. The Genome Analysis Toolkit: a MapReduce framework for analyzing next-generation DNA sequencing data. Genome Res. 20, 1297–1303. https://doi.org/10.1101/gr.107524.110.

Meier, J.I., Marques, D.A., Mwaiko, S., Wagner, C.E., Excoffier, L., Seehausen, O., 2017. Ancient hybridization fuels rapid cichlid fish adaptive radiations. Nat. Commun. 8, 14363. https://doi.org/10.1038/ncomms14363.

Melo-Ferreira, J., Boursot, P., Carneiro, M., Esteves, P.J., Farelo, L., Alves, P.C., 2012. Recurrent introgression of mitochondrial DNA among hares (*Lepus* spp.) revealed by species-tree inference and coalescent simulations. Syst. Biol. 61, 367–381. https://doi.org/10.1093/sysbio/syr114.

Melo-Ferreira, J., Vilela, J., Fonseca, M.M., da Fonseca, R.R., Boursot, P., Alves, P.C., 2014. The elusive nature of adaptive mitochondrial DNA evolution of an arctic lineage prone to frequent introgression. Genome Biol. Evol. 6, 886–896. https://doi.org/10.1093/gbe/evu059.

Meyer, B.S., Matschiner, M., Salzburger, W., 2017. Disentangling incomplete lineage sorting and introgression to refine species-tree estimates for lake Tanganyika cichlid fishes. Syst. Biol. 66, 531–550. https://doi.org/10.1093/sysbio/syw069.

Mikkelsen, E.K., Weir, J.T., 2022. Phylogenomics reveals that mitochondrial capture and nuclear introgression characterizes Skua species proposed to be of hybrid origin. Syst Biol:syac078. https://doi.org/10.1093/sysbio/syac078.

Minh, B.Q., Schmidt, H.A., Chernomor, O., Schrempf, D., Woodhams, M.D., von Haeseler, A., Lanfear, R., 2020. IQ-TREE 2: new models and efficient methods for phylogenetic inference in the genomic era. Mol. Biol. Evol. 37, 1530–1534. https://doi.org/10.1093/molbev/msaa015.

Morales, H.E., Pavlova, A., Amos, N., Major, R., Kilian, A., Greening, C., Sunnucks, P., 2018. Concordant divergence of mitogenomes and a mitonuclear gene cluster in bird lineages inhabiting different climates. Nat. Ecol. Evol. 2, 1258–1267.

Oliveira, E.F., Gehara, M., Sao-Pedro, V.A., Chen, X., Myers, E.A., Burbrink, F.T., Mesquita, D.O., Garda, A.A., Colli, G.R., Rodrigues, M.T., Arias, F.J., Zaher, H., Santos, R.M., Costa, G.C., 2015. Speciation with gene flow in whiptail lizards from a Neotropical xeric biome. Mol. Ecol. 24, 5957–5975. https://doi.org/10.1111/mec.13433.

Oliveira, E.F., Martinez, P.A., Sao-Pedro, V.A., Gehara, M., Burbrink, F.T., Mesquita, D. O., Garda, A.A., Colli, G.R., Costa, G.C., 2018. Climatic suitability, isolation by distance and river resistance explain genetic variation in a Brazilian whiptail lizard. Heredity 120, 251–265. https://doi.org/10.1038/s41437-017-0017-2.

Ortiz, D., Pekar, S., Bilat, J., Alvarez, N., 2021. Poor performance of DNA barcoding and the impact of RAD loci filtering on the species delimitation of an Iberian ant-eating spider. Mol. Phylogenet. Evol. 154, 106997. https://doi.org/10.1016/j.ympev.2020.106997.

Patton, A.H., Margres, M.J., Epstein, B., Eastman, J., Harmon, L.J., Storfer, A., 2020. Hybridizing salamanders experience accelerated diversification. Sci. Rep. 10. https://doi.org/10.1038/s41598-020-63378-w.

Payseur, B.A., Rieseberg, L.H., 2016. A genomic perspective on hybridization and speciation. Mol. Ecol. 25, 2337–2360. https://doi.org/10.1111/mec.13557.

Pedraza-Marrón, C.D.R., Silva, R., Deeds, J., Van Belleghem, S.M., Mastretta-Yanes, A., Domínguez-Domínguez, O., Rivero-Vega, R.A., Lutackas, L., Murie, D., Parkyn, D., Bullock, L.H., Foss, K., Ortiz-Zuazaga, H., Narvaez-Barandica, J., Acero, A., Gomes, G., Betancur, R.R., 2019. Genomics overrules mitochondrial DNA, siding with morphology on a controversial case of species delimitation. Proc. Biol. Sci. 286, 20182924. https://doi.org/10.1098/rspb.2018.2924.

Pickrell, J.K., Pritchard, J.K., 2012. Inference of population splits and mixtures from genome-wide allele frequency data. PLoS Genet. 8, e1002967. https://doi.org/10.1371/journal.pgen.1002967.

Pinho, C., Hey, J., 2010. Divergence with gene flow: models and data. Annu. Rev. Ecol. Evol. Syst. 41, 215–230. https://doi.org/10.1146/annurev-ecolsys-102209-144644.

Quattrini, A.M., Wu, T., Soong, K., Jeng, M.S., Benayahu, Y., McFadden, C.S., 2019. A next generation approach to species delimitation reveals the role of hybridization in a cryptic species complex of corals. BMC Evol. Biol. 19, 116. https://doi.org/10.1186/s12862-019-1427-y.

R Core Team, 2021. R: A language and environment for statistical computing. R Foundation for Statistical Computing, Vienna, Austria https://www.R-project.org/.

Rambaut, A., Drummond, A.J., Xie, D., Baele, G., Suchard, M.A., 2018. Posterior Summarization in Bayesian Phylogenetics Using Tracer 1.7. Syst. Biol. 67, 901–904. https://doi.org/10.1093/sysbio/syy032.

Rand, D.M., Haney, R.A., Fry, A.J., 2004. Cytonuclear coevolution: the genomics of cooperation. Trends Ecol. Evol. 19, 645–653. https://doi.org/10.1016/j.tree.2004.10.003.

Recoder, R.S., Rodrigues, M.T., 2020. Diversification processes in lizards and snakes from the middle São Francisco river dune region, Brazil. In: Rull, V., Carnaval, A. (Eds.), Neotropical Diversification: Patterns and Processes. Fascinating Life Sciences. Springer, Cham, pp. 713–740. https://doi.org/10.1007/978-3-030-31167-4_26.

Reich, D., Thangaraj, K., Patterson, N., Price, A.L., Singh, L., 2009. Reconstructing Indian population history. Nature 461, 489–494. https://doi.org/10.1038/nature08365.

Renaut, S., Grassa, C.J., Yeaman, S., Moyers, B.T., Lai, Z., Kane, N.C., Bowers, J.E., Burke, J.M., Rieseberg, L.H., 2013. Genomic islands of divergence are not affected by geography of speciation in sunflowers. Nat. Commun. 4, 1827. https://doi.org/10.1038/ncomms2833.

Rice, P., Longden, I., Bleasby, A., 2000. EMBOSS: the European molecular biology open software suite. Trends Genet. 16, 276–277. https://doi.org/10.1016/S0168-9525(00)02024-2.

Rodrigues M.T. 2003. Herpetofauna da Caatinga. In: I.R. L., M. T., Silva J.M.C. editors. Ecologia e Conservação da Caatinga. Recife, Editora Universitária da UFPE, p. 181–236.

Romero, P.E., Weigand, A.M., Pfenninger, M., 2016. Positive selection on panpulmonate mitogenomes provide new clues on adaptations to terrestrial life. BMC Evol. Biol. 16, 164. https://doi.org/10.1186/s12862-016-0735-8.

Roux, C., Fraisse, C., Romiguier, J., Anciaux, Y., Galtier, N., Bierne, N., 2016. Shedding light on the grey zone of speciation along a continuum of genomic divergence. PLoS Biol. 14, e2000234. https://doi.org/10.1371/journal.pbio.2000234.

Shtolz, N., Mishmar, D., 2019. The mitochondrial genome–on selective constraints and signatures at the organism, cell, and single mitochondrion levels. Front. Ecol. Evol. 7. https://doi.org/10.3389/fevo.2019.00342.

Shults, P., Hopken, M., Eyer, P.A., Blumenfeld, A., Mateos, M., Cohnstaedt, L.W., Vargo, E.L., 2022. Species delimitation and mitonuclear discordance within a species complex of biting midges. Sci. Rep. 12, 1730. https://doi.org/10.1038/s41598-022-05856-x.

Silva, M.B., Ávila-Pires, T.C.S., 2013. The genus *Cnemidophorus* (Squamata: Teiidae) in state of Piauí, northeastern Brazil, with description of a new species. Zootaxa 3681, 455–477. https://doi.org/10.11646/zootaxa.3681.4.8.

Silva, J.M.C., Leal, I.R., Tabarelli, M., 2017. Caatinga: the largest tropical dry forest region in South America. New York, Springer. https://doi.org/10.1007/978-3-319-68339-3.

Sinha R., Stanley G., Gulati G.S., Ezran C., Travaglini K.J., Wei E., Chan C.K.F., Nabhan A.N., Su T., Morganti R.M., Conley S.D., Chaib H., Red-Horse K., Longaker M.T., Snyder M.P., Krasnow M.A., Weissman I.L. 2017. Index switching causes "spreading-of-signal" among multiplexed samples in Illumina HiSeq 4000 DNA sequencing. bioRxiv. https://doi.org/10.1101/125724.

Sloan, D.B., Havird, J.C., Sharbrough, J., 2017. The on-again, off-again relationship between mitochondrial genomes and species boundaries. Mol. Ecol. 26, 2212–2236. https://doi.org/10.1111/mec.13959.

Solís-Lemus, C., Bastide, P., Ané, C., 2017. PhyloNetworks: a package for phylogenetic networks. Mol. Biol. Evol. 34, 3292–3298. https://doi.org/10.1093/molbev/msx235.

Stenz, N.W., Larget, B., Baum, D.A., Ane, C., 2015. Exploring tree-like and non-tree-like patterns using genome sequences: an example using the inbreeding plant species *Arabidopsis thaliana* (L.) Heynh. Syst. Biol. 64, 809–823. https://doi.org/10.1093/sysbio/syv039.

Stull, G.W., Soltis, P.S., Soltis, D.E., Gitzendanner, M.A., Smith, S.A., 2020. Nuclear phylogenomic analyses of asterids conflict with plastome trees and support novel relationships among major lineages. Am. J. Bot. 107, 790–805. https://doi.org/10.1002/ajb2.1468.

Suchard M.A., Lemey P., Baele G., Ayres D.L., Drummond A.J., Rambaut A. 2018. Bayesian phylogenetic and phylodynamic data integration using BEAST 1.10. Virus Evolution 4:vey016. https://doi.org/10.1093/ve/vey016.

Sun, K., Meiklejohn, K.A., Faircloth, B.C., Glenn, T.C., Braun, E.L., Kimball, R.T., 2014. The evolution of peafowl and other taxa with ocelli (eyespots): a phylogenomic approach. Proc. Biol. Sci. 281. https://doi.org/10.1098/rspb.2014.0823.

Taylor, S.A., Larson, E.L., 2019. Insights from genomes into the evolutionary importance and prevalence of hybridization in nature. Nat. Ecol. Evol. 3, 170–177. https://doi.org/10.1038/s41559-018-0777-y.

Telschow, A., Gadau, J., Werren, J.H., Kobayashi, Y., 2019. Genetic incompatibilities between mitochondria and nuclear genes: effect on gene flow and speciation. Front. Genet. 10. https://doi.org/10.3389/fgene.2019.00062.

Thanou, E., Kornilios, P., Lymberakis, P., Leache, A.D., 2020. Genomic and mitochondrial evidence of ancient isolations and extreme introgression in the four-lined snake. Curr. Zool. 66, 99–111. https://doi.org/10.1093/cz/zoz018.

Tigano, A., Friesen, V.L., 2016. Genomics of local adaptation with gene flow. Mol. Ecol. 25, 2144–2164. https://doi.org/10.1111/mec.13606.

Toews, D.P., Brelsford, A., 2012. The biogeography of mitochondrial and nuclear discordance in animals. Mol. Ecol. 21, 3907–3930. https://doi.org/10.1111/j.1365-294X.2012.05664.x.

Wang, X., Auler, A.S., Edwards, R.L., Cheng, H., Cristalli, P.S., Smart, P.L., Richards, D. A., Shen, C., 2004. Wet periods in northeastern Brazil over the past 210 kyr linked to distant climate anomalies. Nature 432, 740–743. https://doi.org/10.1038/nature03067.

Wang, X., He, Z., Shi, S., Wu, C.I., 2020. Genes and speciation: is it time to abandon the biological species concept? Natl. Sci. Rev. 7, 1387–1397. https://doi.org/10.1093/nsr/nwz220.

Wen, D., Nakhleh, L., 2018. Coestimating reticulate phylogenies and gene trees from multilocus sequence data. Syst. Biol. 67, 439–457. https://doi.org/10.1093/sysbio/syx085.

Werneck, F.P., 2011. The diversification of eastern South American open vegetation biomes: historical biogeography and perspectives. Quat. Sci. Rev. 30, 1630–1648. https://doi.org/10.1016/j.quascirev.2011.03.009.

Werneck, F.P., Gamble, T., Colli, G.R., Rodrigues, M.T., Sites Jr, J.W., 2012. Deep diversification and long-term persistence in the South American 'dry diagonal': integrating continent-wide phylogeography and distribution modeling of geckos. Evolution 66, 3014–3034. https://doi.org/10.1111/j.1558-5646.2012.01682.x.

Wu, C., 2001. The genic view of the process of speciation. J. Evol. Biol. 14, 851–865. https://doi.org/10.1046/j.1420-9101.2001.00335.x.
Yeaman, S., Whitlock, M.C., 2011. The genetic architecture of adaptation under migration-selection balance. Evolution 65, 1897–1911. https://doi.org/10.1111/j.1558-5646.2011.01269.x.
Zerbino, D.R., Birney, E., 2008. Velvet: algorithms for de novo short read assembly using de Bruijn graphs. Genome Res. 18, 821–829. https://doi.org/10.1101/gr.074492.107.
Zhang, C., Rabiee, M., Sayyari, E., Mirarab, S., 2018. ASTRAL-III: polynomial time species tree reconstruction from partially resolved gene trees. BMC Bioinf. 19, 153. https://doi.org/10.1186/s12859-018-2129-y.
Zinenko, O., Sovic, M., Joger, U., Gibbs, H.L., 2016. Hybrid origin of European vipers (*Vipera magnifica* and *Vipera orlovi*) from the Caucasus determined using genomic scale DNA markers. BMC Evol. Biol. 16, 76. https://doi.org/10.1186/s12862-016-0647-7.